Sustainable Convergence of Electricity and Transport Sectors in the Context of a Hydrogen Economy

Amir H. Hajimiragha[a,*], Claudio A. Cañizares[a], Michael W. Fowler[b], Somayeh Moazeni[c], Ali Elkamel[b], Steven Wong[a]

[a] *Power and Energy Systems Group, Department of Electrical and Computer Engineering, University of Waterloo, 200 University Avenue West, Waterloo, Ontario, Canada N2L 3G1*
[b] *Department of Chemical Engineering, University of Waterloo, 200 University Avenue West, Waterloo, Ontario, Canada N2L 3G1*
[c] *Cheriton School of Computer Science, Faculty of Mathematics, University of Waterloo, 200 University Avenue West, Waterloo, Ontario, Canada N2L 3G1*

Abstract

This paper analyzes the electricity and transport sectors within a single integrated framework and presents the capabilities of this integrated approach to realize an environmentally and economically sustainable transport sector based on fuel cell vehicles (FCVs). A comprehensive robust optimization planning model for the transition to FCVs is developed, considering the constraints of both electricity and transport sectors. These models are finally applied to the real case of Ontario, Canada to determine the Ontario's grid potential to support these vehicles in the transport sector for a planning horizon ending in 2025. With a reasonable trade-off between optimality and conservatism, it is found that more than 170,000 FCVs can be introduced into Ontario's transport sector by 2025 without jeopardizing the reliability of the system or any additional grid investments such as new power generation installations.

Keywords: Hydrogen economy, fuel cell vehicle, transportation, electric grid, planning, uncertainty, robust optimization, Ontario

Abbreviations

AFV Alternative-Fuel Vehicle.

FCV Fuel Cell Vehicle.

GV Gasoline Vehicle.

HHV Higher Heating Value.

HOEP Hourly Ontario Energy Price.

HPP Hydrogen Production Plant.

IESO Independent Electricity System Operator.

LDV Light-duty Vehicle.

*Corresponding author, Tel: 1-519-888-4567 ext. 38036; Fax: 1-519-746-3077
Email addresses: ahajimir@uwaterloo.ca (Amir H. Hajimiragha), ccanizares@uwaterloo.ca (Claudio A. Cañizares), mfowler@cape.uwaterloo.ca (Michael W. Fowler), smoazeni@math.uwaterloo.ca (Somayeh Moazeni), aelkamel@uwaterloo.ca (Ali Elkamel), sm2wong@engmail.uwaterloo.ca (Steven Wong)

$MILP$ Mixed Integer Linear Programming.

NE Northeast.

NW Northwest.

SCC Social Cost of Carbon.

SW Southwest.

Nomenclature

Indices

c Index for vehicle type.

e Index for constraint under uncertainty.

i, j Index for zones.

l Index for voltage angle block.

m Index for Monte Carlo simulation.

v Index for uncertain parameter.

y, k Index for year.

τ, ω Index for time period.

ω_1 Index for the time period corresponding to weekday hours.

ω_2 Index for the time period corresponding to weekend hours.

Sets

E Set of constraints subject to uncertainty.

L_1 Set of total voltage angle blocks; L_1=$\{1, ..., L\}$.

L_2 Set of voltage angle blocks; L_2=$\{1, ..., L-1\}$.

L_3 Set of voltage angle blocks; L_3=$\{2, ..., L\}$.

L_4 Set of voltage angle blocks; L_4=$\{2, ..., L-1\}$.

U Set of uncertainty.

V Set of total uncertain parameters.

V_e Set of uncertain parameters in constraint e.

VT Set of different types of light-duty vehicles.

X Set of mixed integer feasible solution.

Y Set of planning years.

Y_1 Set of planning years excluding the first year.

Z Set of zones.

Z^* Set of hydrogen transfer corridors.

Ψ Set of time periods; $\Psi = \{\omega_1, \omega_2\}$.

Ω Set of transmission lines.

Parameters

AM Annual mileage (km).

b_{ijy} Line susceptance (p.u.).

CC_{cab} Capital cost of cab (CAD).

CC_{tube} Capital cost of tube trailers (CAD).

Cf_y Correction factor.

CF_{hpp} Average capacity factor of HPPs (%).

$Chpp_{iy}$ Local required capacity of HPPs (MW).

$\overline{CT}$ Maximum capacity of each compressed gas truck (ton).

d_{ij} Approximate distance between zones (km).

DR Discount rate (%).

E_{CO_2} Constant value of CO_2 emissions from burning gasoline (kg/litre).

ER_{chp_i} Emission rate of CHP plants (ton/MWh).

ER_{coal_i} Emission rate of coal plants (ton/MWh).

FE_{fcv} Fuel economy of the fuel cell vehicle (km/kg).

$FE_{gv_{cy}}$ Fuel economy of the gasoline vehicle (km/litre).

g_{ijy} Line conductance (p.u.).

h Number of off-peak hours.

h_{wd} Number of HPPs operation hours in weekdays.

h_{we} Number of HPPs operation hours in weekends.

H Last year of the planning horizon.

HHV Higher heating value of hydrogen (kWh/kg).

L Total number of voltage angle blocks.

LF Linking factor (ton/day.MW).

LT_{cab} Lifetime of cab (year).

LT_{tube} Lifetime of tube trailer (year).

M Number of Monte Carlo simulations.

$Nldv_{iy}$ Total number of light-duty vehicles.

OC_y Operation cost of compressed gas truck (CAD/km).

p_e Threshold probability of constraint e.

P_{e_y} Total base-load electricity demand (MW).

$P^{\tau}_{e_{iy}}$ Zonal base-load electricity demand (MW).

$\overline{P_{g_{iy}}}$ Maximum available generation power (MW).

$\underline{P_{g_{iy}}}$ Lower bound of zonal generation power (MW).

$\overline{P_{ga}}_{iy}$ Maximum capacity of non-polluting generation resources (MW).

$\overline{P_{gb}}_{iy}$ Maximum capacity of non-polluting plus CHP generation resources (MW).

$\overline{P_{hpp}}_{iy}$ Maximum size of HPPs (MW).

$\overline{P_{m}}_{iy}$ Upper bound of imported power (MW).

$\underline{P_{m}}_{iy}$ Lower bound of imported power (MW).

$\overline{P_{x}}_{iy}$ Upper bound of exported power (MW).

$\underline{P_{x}}_{iy}$ Lower bound of exported power (MW).

$\overline{Pd}_{ijy}$ Maximum capacity of transmission corridor for direct power flow (MW).

$\overline{Pr}_{ijy}$ Maximum capacity of transmission corridor for reverse power flow (MW).

PS Planning span (year).

s_{ev} Scaled deviation.

S_{cab_y} Salvage value of cab (% of initial cost).

S_{tube_y} Salvage value of tube trailer (% of initial cost).

$SC_{CO_2}p$ Social cost of CO_2 emission in the population area (CAD/ton).

$SC_{CO_2}g$ Social cost of CO_2 emission of generation (CAD/ton).

$\overline{TH}$ Upper bound of transferred hydrogen (ton/day).

$\underline{TH}$ Lower bound of transferred hydrogen (ton/day).

VS_c Percent share of vehicle.

y_1 First year of the planning horizon.

$\alpha_{ijy}(l)$ Slope of the lth block of voltage angle (MW/rad).

Γ_e Budget of uncertainty.

$\Delta\delta_y$ Upper bound of each angle block (rad).

$\Delta\eta_{hpp}$ Efficiency improvement of the HPPs over the planning horizon.

$\overline{\Delta P_{hpp}}_{iy}$ Maximum annual development of HPPs (MW).

ϵ_a, ϵ_b Small positive numbers.

ε_t Constraint violation probability (%).

η^b_{hpp} Base efficiency of HPPs at the beginning of the planning horizon.

λ A random parameter following a normal distribution with zero mean and unit standard deviation.

$\bar{\mu}_y$ Maximum possible FCV penetration (%).

π_y Internal or hourly Ontario energy price (CAD/MWh).

π_{m_y} Import electricity price (CAD/MWh).

π_{x_y} Export electricity price (CAD/MWh).

ρ Size of the relative perturbation (%).

Variables

FF_{iy} Feasibility factor.

K^{τ}_{liy} Binary variable to denote if the average zonal generation power is located in the lth segment of the emission cost curve ($l = 1, 2, 3$).

N_{ijy} Integer number of required compressed gas trucks or tube trailers with the capacity of $\overline{CT}$.

NT_y Total number of compressed gas trucks or tube trailers with the capacity of $\overline{CT}$.

p_e, q_{ev}, r_v Additional continuous variables used to develop robust counterpart problems.

$P^{\tau}_{g_{iy}}$ Average zonal generation power (MW).

$P^{\tau}_{gl_{iy}}$ Continuous auxiliary variable for the average zonal generation power ($l = 1, 2, 3$).

$P^{\tau}_{l_{iy}}$ Total base-load electricity demand including HPPs (MW).

$P_{m_{iy}}$ Zonal imported power (MW).

$P_{x_{iy}}$ Zonal exported power (MW).

PC_k Integer number of purchased cabs.

Ph_{iy} Local required capacity of HPPs (MW).

$Phpp_{iy}$ Total installed HPP capacity (MW).

$Ploss_{ij}$ Power loss (MW).

Ps_{ijy} Contribution of zone i in total required power of HPPs in zone j (MW).

PT_k Integer number of purchased compressed gas trucks or tube trailers with the capacity of $\overline{CT}$.

TH_{ijy} Transferred hydrogen (ton/day).

V^{τ}_{liy} Continuous auxiliary variable for $K^{\tau}_{liy}P^{\tau}_{g_{iy}}$ ($l = 1, 2, 3$).

W Continuous variable used to represent all the uncertain parameters in the constraints of the robust counterpart problem.

β_{ijy} Binary variable to denote if there is transferred hydrogen between zones.

δ^{τ}_{iy} Voltage angle (rad).

δ^{τ}_{ijy} Voltage angle difference (rad).

$\delta^{\tau}_{ijy}(l)$ Value of the lth block of voltage angle (rad).

$\delta^{\tau+}_{ijy}$, $\delta^{\tau-}_{ijy}$ Nonnegative variables used to linearize the absolute value $\left|\delta^{\tau}_{iy} - \delta^{\tau}_{jy}\right|$ (rad).

$\mu^{\tau}_{ijy}(l)$ Binary variable to denote if the value of the lth voltage angle block is equal to its maximum value $\Delta\delta_y$.

1. Introduction

1.1. Motivation

The transport sector is one of the largest and fastest growing contributors to both energy demand and greenhouse gases; for example, in Canada, the transport sector represents almost 35% of the total energy demand and is the second highest source of greenhouse gas emissions [1, 2]. In view of these facts and the challenges associated with the supply of oil, the issue of alternative fuels for meeting the future energy demand of the transport sector has gained notable attention.

The efficient utilization of the existing infrastructure should be first considered to address the significant increase of energy demand and environmental concerns. For example, the electric grid is designed to meet the highest expected demand, which occurs at most about 5% of the time. For the remaining time, in particular during off-peak hours, namely 11 pm to 7 am, the system is underutilized and could generate and deliver a substantial amount of energy to other sectors such as transport without jeopardizing the reliability of the system. This unutilized generation capacity can be used efficiently in electrolytic hydrogen production for use by FCVs.

Hydrogen fuel is a zero-emission option for light-duty vehicles, especially in urban centers where air quality is an issue. Furthermore, the introduction of FCVs into the transport sector improves the utilization and efficiency of the existing electricity grids and also helps for further development of renewable energy sources in the future. Thus, the environmental benefits of renewable energy sources such as wind and solar are sometimes overshadowed by their intermittent nature and resulting low capacity factors; this makes the development of these resources a challenging task, and necessitates an energy storage or load leveling option. However, the storage capacity of hydrogen in FCVs provides dispersed storage capacity for the whole grid that could help address this intermittency issue for the benefit of the transport sector, based on a more wholistic energy management approach.

With regard to the challenges associated with fueling the transport sector and environmental benefits of FCVs as well as the technical advantages of electric drives, FCVs are expected to have profound impact on future transport sectors. Therefore, development of analytical tools in the context of a hydrogen economy for planning the transition to these vehicles is of great importance.

1.2. Literature Review and Methodology

The hydrogen economy is defined as a future economy in which hydrogen is adopted for mobile applications and electric grid load balancing [3]–[6]. The hydrogen economy that is considered in this study is based solely on electrolytic hydrogen production during off-peak periods for use of FCVs. Note that there has been much criticism of the potential for a hydrogen economy, because most of the analyses of the transition to a hydrogen economy include future and unproven technologies that are not yet commercialized. Thus, the scope of this study is restricted to commercially available and well-established technologies such as electrolysis in order to provide a more realistic analysis of the transition to this economy.

Earlier works have presented studies of the potential penetration of plug-in hybrid electric vehicles based on off-peak charging periods (e.g., see [7]). Clearly, the transition to zero-emission LDVs cannot be met with battery vehicles alone because of their limitation with respect to vehicle range, recharge time and battery durability. Thus, the present work addresses the potential of hydrogen production for a transition to full-range zero-emission vehicles, demonstrating that hydrogen vehicles can be part of a zero-emission fleet.

Economic assessment of electrolytic hydrogen production as a whole, independent of the type of power source for the HPPs, is studied in [8] where electricity prices and fuel taxes are shown to be the two dominant factors influencing the competitive position of electrolytic hydrogen production. The cost of electrolytic hydrogen production, particularly during off-peak periods, has been studied in [9], considering different fluctuating and stable electricity markets. It is shown in [9] that hydrogen production using off-peak electricity, where prices are sufficiently low, can be of interest in those countries that have highly fluctuating electricity spot markets.

Solar or wind-based hydrogen production to meet the demands of FCVs has been studied in a number of papers (e.g., [10]–[13]), where the main emphasis is on the role of hydrogen in the transport sector to

overcome the intermittency issues of these resources. These studies typically rely on a single type of power generation resource and do not consider the mix of different available generation resources to support a hydrogen economy. Although renewable energy resources such as wind and solar can help to meet the requirement of a true hydrogen economy, neglecting other low-polluting generation resources causes power system planners to underestimate the grid potential for covering the hydrogen requirements of FCVs.

Planning the transition to a hydrogen economy has been studied in various locations and reported in the literature [14]–[26]. Each of these plans considers particular aspects of this issue, varying considerably from place to place due to different local limitations and energy policies, and with inadequate attention to the electric grid constraints. This paper explores a different aspect of a hydrogen economy transition in the transport sector by developing an optimization planning model that takes into account both electricity and hydrogen networks as one integrated system, while considering a host of uncertainties. The proposed model considers the future development of both generation and transmission systems within a planning horizon, and determines the optimal size of HPPs to be installed in different locations and the optimal hydrogen transportation routes required to achieve optimal hydrogen economy penetrations during this planning framework. Furthermore, based on the reported works (e.g., [16, 20]), planning the transition to a hydrogen economy is usually based on some estimates of hydrogen economy penetrations at a fixed time in the future; however, the optimal values of these penetrations are determined in the proposed model via an optimization process. These optimal values are influenced by the electric grid constraints as well as by hydrogen transfer limits.

1.3. Objectives and Contributions

Motivated by the notion of efficient utilization of the existing infrastructure, this paper aims to develop a comprehensive optimization model for planning the transition to FCVs. This optimization framework determines the optimal electric grid potential to accommodate FCVs during a planning horizon taking into account the environmental issues in both transport sector and generation facilities. The proposed model is applied to Ontario, Canada, to determine the optimal potential penetrations of FCVs into Ontario's transport sector, based on the existing electric grid infrastructure and future plans for its development, and without any additional grid investment to specifically support FCVs. Due to lack of detailed information regarding the structure of the Ontario's electricity grid with regard to generation and transmission beyond 2025, this analysis concentrates on studying a planning horizon ending in 2025. However, the proposed methodology can be applied to any medium or long-term planning horizons, depending on the availability of reliable planning data.

The conceptual vision of the research presented in this paper is shown in Fig. 1, which depicts the main sub-models, required data, analytical engine and major results. As can be observed in Fig. 1, the proposed optimization model involves many parameters that must be estimated; however, estimation errors may substantially influence the optimal solution. In order to resolve this problem, the application of a robust optimization approach for planning the transition to FCVs is proposed. Thus, a sensitivity analysis using Monte Carlo simulation is performed to find the impact of estimation errors in the parameters of the planning model; the results of this study reveals the most influential uncertain parameters on the optimal solution. These parameters are then used to develop a robust planning model. This model allows decision makers to adjust the level of conservatism, and address the shortcoming of the classic robust optimization approach, where robustness is ensured at the cost of significant loss of optimality. It should be emphasized that the incorporation of the most relevant uncertainties into the model and presenting the robust optimization analysis along with the real-case example of Ontario, Canada, are all attempts to introduce a more realistic hydrogen economy scenario.

The proposed model in this paper builds upon the authors' previous work reported in [27] with the following new contributions:

1. An appropriate model of generation emission cost is developed to factor in the environmental consequences of FCVs.
2. A comprehensive model of hydrogen transportation between different zones is developed.

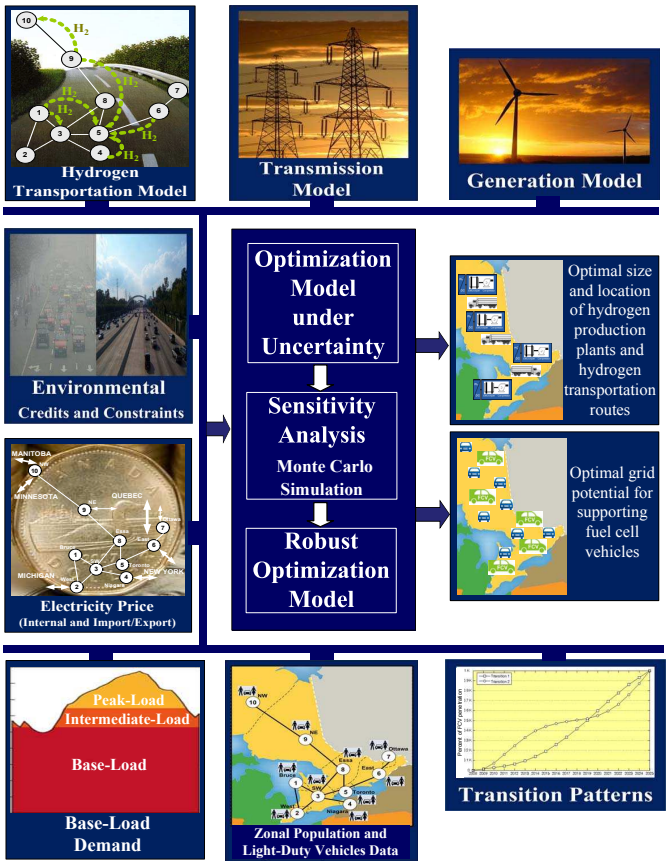

Figure 1: An overview of the research concept.

3. A methodology based on Monte Carlo simulation is proposed and implemented to study the issue of parameter uncertainty, and to derive the most influential parameter uncertainties based on their impacts on the optimal value.
4. A robust optimization approach is applied using the most influential uncertain parameters to derive robust optimal penetrations of FCVs into the transport sector with application to Ontario, Canada.

The remainder of the paper is structured as follows: In Section 2, environmental aspects of FCVs in both transport sectors and generation sites are comprehensively discussed, followed by developing an emission cost model of generation. Section 3 presents a detailed optimization framework for planning the transition to FCVs by first developing an enhanced hydrogen transportation model. Section 4 discusses the impact of parameter uncertainty in optimization models, and the methodologies used to deal with this problem; the robust optimization approach adopted in this study to address the issue of data uncertainty is briefly reviewed in this section. The application of the proposed optimization model to Ontario, Canada is presented in Section 5, followed by a comprehensive sensitivity analysis to identify and rank the most influential parameters. The application of the robust optimization approach for planning the transition to FCVs in this case that properly accounts for the most relevant uncertainties is discussed in this section. Finally, Section 6 summarizes the main conclusions and contributions of the present study.

2. Environmental Impacts of FCVs

Many attempts have been made thus far to assign a monetary value to the damage caused by CO_2 emissions, which is commonly referred to as the social cost of carbon (SCC). More precisely, it is an estimate

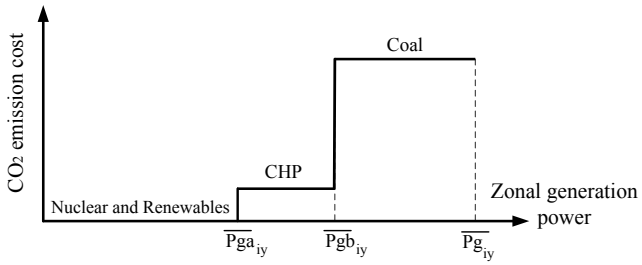

Figure 2: Emission cost function of generation.

of the economic value of the extra or marginal impact caused by the emission of one more tonne of carbon (in the form of CO_2) at any point in time [28]. The SCC can also be interpreted as the marginal benefit of reducing carbon emissions by one tonne [29]. Reported values in the literature for the SCC come in an extremely wide range. As an example, the probability function developed in [30] based on 100 estimates of the SCC from 28 published studies, displays a median of 14 USD/ton of carbon, a mean of 93 USD/ton, and a 95th percentile estimate equal to 350 USD/ton. There are also other estimates of the SCC running from less than 1 USD/ton to over 1500 USD/ton of carbon [29].

Gasoline and diesel-fuelled vehicles and fossil fuel power plants release CO_2 to the atmosphere; hence, based on SCC, the monetary value of the damages to the environment caused by such vehicles or generation plants can be estimated. Therefore, an environmental credit can be assigned to each FCV that can be introduced to the transport sector in this study, whose value depends on the SCC, the fuel economy of the LDV, that is being replaced by a FCV, and the known value of CO_2 emission from burning gasoline (2.3 kg/litre). An environmental cost is also assigned to each polluting generation plant that is based on the SCC, the power generation level, and the CO_2 emission rates of the plant. Disregarding this type of environmental cost may lead to overestimating the environmental benefits of FCVs; thus, in order to cover the energy requirement of the FCVs, extra power must be generated by generation facilities which may not necessarily be a renewable source of energy. Therefore, while adopting FCVs in the transport sector reduces the CO_2 emission in the population area where the vehicle is used, it may increase the CO_2 emission from power generation, depending on the share of fossil fuel in the marginal generation mix.

Although high penetration of FCVs may not necessarily result in emission reductions in all regions, it would help to shift the emission from millions of tailpipes in highly populated areas to a limited number of central generation power plants, thus facilitating more efficient control and management of CO_2 emissions. Therefore, as per [31], this study differentiates the impact of CO_2 emissions based on point of origin, and roughly assumes that the environmental credit of one ton CO_2 cut in densely populated areas is substantially larger than the environmental cost of one ton CO_2 increase in sparsely populated areas where most large power plants are typically located. This assumption is mainly based on the fact that the environmental benefits of FCVs are not limited to CO_2 emission reductions, since the greenhouse gas emissions are also correlated with urban air emissions such as photochemical smog, volatile organic compound, particulate matters, NO_x, SO_x and Hg. These emissions are much more significant in densely populated areas, and all these could be reduced by the introduction of FCVs into the transport sector [32]. Thus, in this study, all these impacts are approximately captured in different social cost values of CO_2 emissions in the transport sector and generation power plants [33].

Based on the aforementioned discussions, CO_2 emission costs of generation are considered in the optimization model for transition to FCVs. Figure 2 represents a typical emission cost function during off-peak hours, when the contributing generation resources include nuclear, renewables, CHP and coal plants; it is to be noted that the contribution of gas-fired generation is not usually considered during off-peak hours. The emission cost function represented in this figure in zone i and year y during the time period of τ, which

corresponds to off-peak hours, can be expressed as follows:

$$EC_{iy}=\begin{cases} 0 & 0 \le P^{\tau}_{g_{iy}} \le \overline{P_{ga}}_{iy} \\ ER_{chp_i}\left(P^{\tau}_{g_{iy}} - \overline{P_{ga}}_{iy}\right) & \\ \times SC_{CO_2} g \times h \times 365 & \overline{P_{ga}}_{iy} < P^{\tau}_{g_{iy}} \le \overline{P_{gb}}_{iy} \\ \left[ER_{chp_i}\left(\overline{P_{gb}}_{iy} - \overline{P_{ga}}_{iy}\right) + ER_{coal_i}\left(P^{\tau}_{g_{iy}} - \overline{P_{gb}}_{iy}\right)\right] & \\ \times SC_{CO_2} g \times h \times 365 & \overline{P_{gb}}_{iy} < P^{\tau}_{g_{iy}} \le \overline{P_{g}}_{iy} \end{cases} \quad (1)$$

In order to incorporate cost function (1) into the optimization model, three sets of binary variables K^{τ}_{1iy}, K^{τ}_{2iy} and K^{τ}_{3iy} corresponding to three segments of the cost function in Fig. 2 are defined. Also, three sets of continuous auxiliary variables $P^{\tau}_{g_{1iy}}$, $P^{\tau}_{g_{2iy}}$ and $P^{\tau}_{g_{3iy}}$ for the average zonal generation power $P^{\tau}_{g_{iy}}$ are needed, which are defined as follows:

$$P^{\tau}_{g_{iy}} = \begin{cases} P^{\tau}_{g_{1iy}} & \text{if } K^{\tau}_{1iy} = 1 \\ P^{\tau}_{g_{2iy}} & \text{if } K^{\tau}_{2iy} = 1 \\ P^{\tau}_{g_{3iy}} & \text{if } K^{\tau}_{3iy} = 1 \end{cases} \quad (2)$$

Based on these sets of binary and continuous auxiliary variables, the incorporation of CO_2 emission costs in the generation side requires the addition of the following cost components into the objective function:

$$\begin{aligned} EC^{*}=\sum_{y}\sum_{i}\Big\{ & ER_{chp_i}\Big[K^{\tau}_{2iy}P^{\tau}_{g_{iy}} - K^{\tau}_{2iy}\overline{P_{ga}}_{iy} + K^{\tau}_{3iy}\Big(\overline{P_{gb}}_{iy} - \overline{P_{ga}}_{iy}\Big)\Big] \\ & + ER_{coal_i}\Big(K^{\tau}_{3iy}P^{\tau}_{g_{iy}} - K^{\tau}_{3iy}\overline{P_{gb}}_{iy}\Big)\Big\} SC_{CO_2} g \times h \times 365 \end{aligned} \quad (3)$$

and the following additional constraints:

$$\begin{aligned} & 0 \le P^{\tau}_{g_{1iy}} \le K^{\tau}_{1iy}\overline{P_{ga}}_{iy} \\ & K^{\tau}_{2iy}\left(\overline{P_{ga}}_{iy} + \epsilon_a\right) \le P^{\tau}_{g_{2iy}} \le K^{\tau}_{2iy}\left(\overline{P_{gb}}_{iy} + \epsilon_a\right) \\ & K^{\tau}_{3iy}\left(\overline{P_{gb}}_{iy} + \epsilon_a + \epsilon_b\right) \le P^{\tau}_{g_{3iy}} \le K^{\tau}_{3iy}\left(\overline{P_{g}}_{iy} + \epsilon_a + \epsilon_b\right) \\ & K^{\tau}_{1iy} + K^{\tau}_{2iy} + K^{\tau}_{3iy} \le 1 \\ & P^{\tau}_{g_{iy}} = P^{\tau}_{g_{1iy}} + P^{\tau}_{g_{2iy}} + P^{\tau}_{g_{3iy}} \\ & \forall i \in Z \wedge y \in Y \wedge \tau \in \Psi \end{aligned} \quad (4)$$

In order to remove non-linear terms in (3), i.e., $K^{\tau}_{2iy}P^{\tau}_{g_{iy}}$ and $K^{\tau}_{3iy}P^{\tau}_{g_{iy}}$, to keep the model an MILP problem, these are replaced by new variables V^{τ}_{2iy} and V^{τ}_{3iy}, respectively, and the following additional constraints:

$$\begin{aligned} & V^{\tau}_{2iy} \ge P^{\tau}_{g_{iy}} - \overline{P_{g}}_{iy}\left(1 - K^{\tau}_{2iy}\right) \\ & V^{\tau}_{3iy} \ge P^{\tau}_{g_{iy}} - \overline{P_{g}}_{iy}\left(1 - K^{\tau}_{3iy}\right) \\ & V^{\tau}_{2iy} \ge \underline{P_{g}}_{iy}K^{\tau}_{2iy} \\ & V^{\tau}_{3iy} \ge \underline{P_{g}}_{iy}K^{\tau}_{3iy} \\ & \forall i \in Z \wedge y \in Y \wedge \tau \in \Psi \end{aligned} \quad (5)$$

3. Optimization Model for Transition to FCVs

In this section, an optimization planning model is developed that takes into account both electricity and hydrogen networks as one integrated system. The purpose of the proposed optimization model is to determine the optimal size of HPPs to be installed in geographically differentiated power generation zones, as well as to find the optimal hydrogen transportation routes to achieve optimal hydrogen economy or FCV penetrations for each year of the planning horizon. This section begins with the development of a hydrogen transportation model, followed by the description of the MILP model.

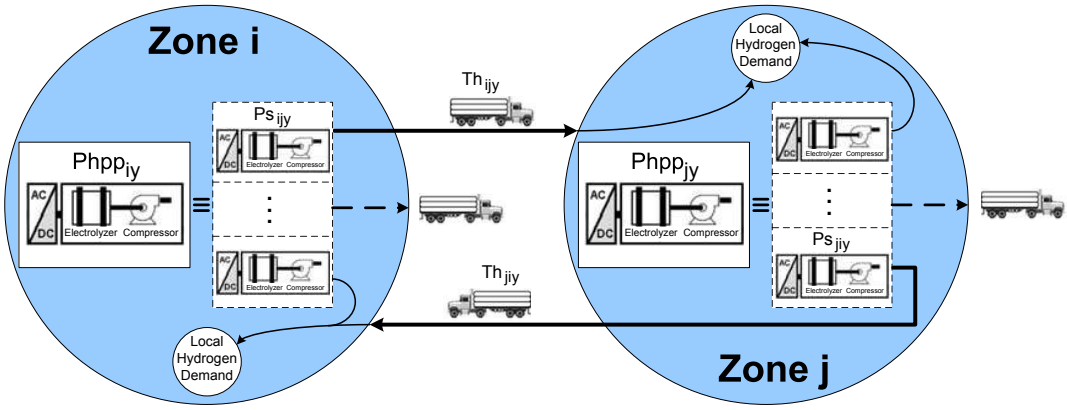

Figure 3: Demonstration of the proposed hydrogen transfer concept.

3.1. Hydrogen Transportation Model

In an ideal case, each zone should be able to fulfill its own hydrogen requirement. However, due to resource limitations in some zones, power loss and congestion in transmission networks, the assumed level of hydrogen economy penetration, and some other operational or placement constraints, there may be a need for hydrogen transfer between particular zones in certain years. Therefore, hydrogen transportation is considered as a replacement for unavailable electric power transmission (electricity transfer) between particular zones.

Among the possible modes of hydrogen transfer, i.e., compressed gas trucks, cryogenic tanker trucks and pipelines [34], the first mode is selected at this stage, mainly due to the considered planning horizon (medium to long term), as well as economic considerations and greater availability and scalability of the required infrastructure compared to other options. This choice can be further justified based on the fact that most of the zonal hydrogen demand is generated locally, and thus the volume of transferred hydrogen is not expected to be significant. Thus, a simple demonstration of the proposed hydrogen transfer concept is shown in Fig. 3, where both hydrogen import and export possibilities exist for each zone. In general, the total installed HPP capacity in zone i, by year y ($Phpp_{iy}$) can be partly utilized for covering the local hydrogen demand as well as the hydrogen requirements of other zones. Hence, the total capacity of an HPP can be decomposed into multiple components, each of which covers a portion of the hydrogen requirement of other zones. For example, the power component Ps_{ijy} in Fig. 3 can be interpreted as the contribution of zone i in total required power of HPPs in zone j, which should be transferred to zone j by compressed gas trucks. Similarly, other zones such as zone j can share the required power of HPPs in zone i based on a power component Ps_{jiy}. Therefore, the required MW capacity of HPPs for zone i by Year y (Ph_{iy}) which supplies the local hydrogen demand to achieve a certain level of hydrogen economy penetration, can be expressed as follows:

$$Ph_{iy} = Phpp_{iy} - \sum_{j \neq i} Ps_{ijy} + \sum_{j \neq i} Ps_{jiy} \qquad \forall i, j \in Z \wedge y \in Y_1 \tag{6}$$

Furthermore, the total installed HPP in zone i by year y is equal to the previously installed HPP by year $y-1$ and the newly installed HPP in year y ($\Delta Phpp_{iy}$), which can be expressed as follows:

$$Phpp_{iy} = Phpp_{iy-1} + \Delta Phpp_{iy} \qquad \forall i \in Z \wedge y \in Y_1 \tag{7}$$

In general, the local required MW capacity of HPPs in zone i and year y for a 100% hydrogen economy

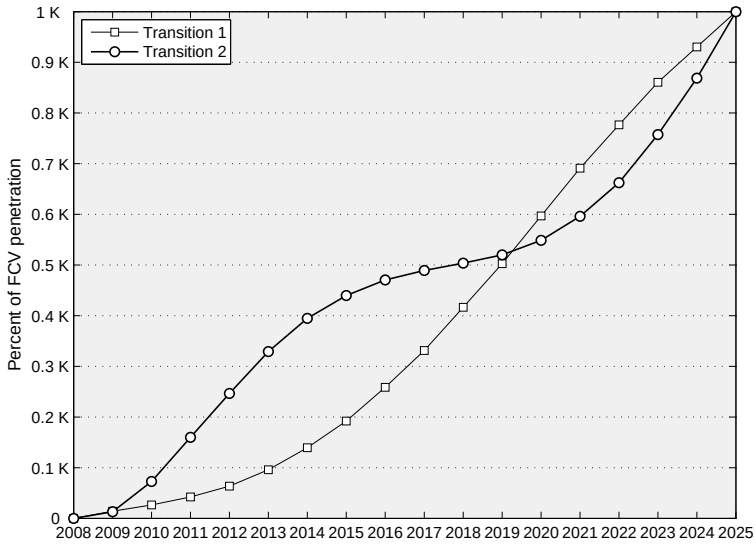

Figure 4: Market penetration of FCVs based on two assumed transitions: 1) rapid early adoption; 2) slow early adoption.

penetration can be calculated as follows:

$$Chpp_{iy} = \frac{10^{-3} AM.HHV}{24 \times 365 \eta^{b}_{hpp}.FE_{fcv}.CF_{hpp}} Cf_y Nldv_{iy} \quad \forall i \in Z \wedge y \in Y \tag{8}$$

where Cf_y is the correction factor in year y, which considers the efficiency improvement of the HPPs over the planning years and is calculated as follows:

$$Cf_y = \frac{\eta^{b}_{hpp}}{\left[\eta^{b}_{hpp} + \frac{\Delta\eta_{hpp}}{PS}\left(y - y_1\right)\right]} \quad \forall y \in Y \tag{9}$$

Based on the definition of $Chpp_{iy}$, the local required MW capacity of HPP to achieve a certain level of hydrogen economy penetration can then be expressed as follows:

$$Ph_{iy} = FF_{iy}\overline{\mu}_y Chpp_{iy} \quad \forall i \in Z \wedge y \in Y \tag{10}$$

Note that $\bar{\mu}_y$, which is the maximum possible hydrogen economy penetration in year y, is fixed by the system planner based on an assumed transition curve as shown in Fig. 4, where $K = 100$ represents a 100% FCV penetration into the transport sector. These transition curves account for the time needed for the development of the required infrastructure and specifies the maximum penetration levels that can be realized in each year to achieve a certain penetration level by the end of the planning horizon. Also, FF_{iy} determines the percentage of the penetration levels set by the transition curve that is achievable due to electricity grid constraints.

Combining (8)-(10) with (6) results in the following equality constraints in which penetration levels are

reflected:

$$Phpp_{iy} - \sum_{j \neq i} Ps_{ijy} + \sum_{j \neq i} Ps_{jiy} - \frac{10^{-3} AM.HHV.Nldv_{iy} \overline{\mu}_y FF_{iy}}{24 \times 365 FE_{fcv} CF_{hpp} \left[\eta^b_{hpp} + \frac{\Delta \eta_{hpp}}{PS}(y - y_1)\right]} = 0 \quad \forall i \in Z \wedge y \in Y_1 \tag{11}$$

As previously discussed and demonstrated in Fig. 3, for each power component Ps_{ijy} (MW) there is a transferred hydrogen component TH_{ijy} (ton/day). These variables can be coupled together by a linking factor LF_y as follows:

$$TH_{ijy} = LF_y Ps_{ijy} \quad \forall (i,j) \in Z^* \wedge y \in Y_1 \tag{12}$$

where $Z^* = \{(i,j) : i,j \in Z, i \neq j\}$ is the set of indices of hydrogen transfer corridors. This relation means that the Ps_{ijy} (MW) component in zone i is capable of producing $LF_y Ps_{ijy}$ (ton/day) hydrogen to be transferred to zone j by compressed gas trucks. In order to find LF_y, one should note the HHV of hydrogen as well as the efficiency and average capacity factor of HPPs; thus, considering the efficiency improvement of HPPs over time, LF_y can, in general, be expressed as follows:

$$LF_y = \frac{24 CF_{hpp}}{HHV}\left[\eta^b_{hpp} + \frac{\Delta \eta_{hpp}}{PS}(y - y_1)\right] \quad \forall y \in Y_1 \tag{13}$$

The average daily transferred hydrogen between zones i and j in each year (TH_{ijy}) should be zero or lie between predefined lower and upper bounds. This requirement can be implemented by defining new binary variables in the following constraint:

$$\beta_{ijy} \underline{TH} \leq TH_{ijy} \leq \beta_{ijy} \overline{TH} \quad \forall (i,j) \in Z^* \wedge y \in Y_1 \tag{14}$$

Depending on the values of transferred hydrogen, appropriate numbers of compressed gas trucks including cabs and tube trailers must be purchased. This can be realized by the following set of constraints:

$$N_{ijy} \geq TH_{ijy} / \overline{CT} \quad \forall (i,j) \in Z^* \wedge y \in Y_1 \tag{15}$$

$$NT_y \geq \sum_{(i,j) \in Z^*} N_{ijy} \quad \forall y \in Y_1 \tag{16}$$

$$\sum_{k=y_1}^{y} PT_k \geq NT_y \quad \forall y \in Y_1 \tag{17}$$

$$\sum_{k=y-LT_{cab}+1}^{y} PC_k = NT_y \quad \forall y \in \{y_1 + LT_{cab} - 1, ..., H\} \tag{18}$$

$$\sum_{k=y_1}^{y} PC_k = NT_y \quad \forall y \in \{y_1, ..., y_1 + LT_{cab} - 1\} \tag{19}$$

Note that the trucks are represented here in two components, i.e., cabs and tube trailers, given the difference in the operational lifetime between them. The required number of compressed gas trucks is linked to the transferred hydrogen in route (i,j) in year y through the constraints (15). Constraints (16) state that the total number of required trucks should not be less than the required trucks in all the possible routes. The total number of purchased trucks (tube trailers) by year y is related to the total number of required trucks

in year y by constraints (17). Constraints (18) and (19) state that the total number of purchased cabs in any time interval equal to the lifetime of the cab ending in year y should be equal to the total number of trucks (tube trailers) needed in year y.

It should be emphasized that the impact of the transport trucks is not taken into account in terms of additional CO_2 emissions. This is justified based on the fact that the number of required trucks is significantly less than the total number of LDVs. This is further clarified in Section 5 where the real-case example of Ontario, Canada, is studied.

3.2. Objective Function

The model's objective is to minimize the present value of the net electricity, emission and hydrogen transportation costs. Thus, the objective function consists of electricity generation and imported/exported power cost/revenue components; emission cost and credit components in generation facilities and population areas, respectively; and the hydrogen transportation costs. Therefore, the objective function can be expressed as follows:

$$\min \sum_{y \in Y} \frac{1}{(1+DR)^{y-y_1}} \left(C_{1y} - C_{2y} + C_{3y} + C_{4y}\right) \tag{20}$$

where $C_{iy}, i \in \{1, ..., 4\}$ are different cost or revenue components, which are defined next.

3.2.1. Net Electricity Cost

C_{1y} represents the net total electricity costs in year y. Since different time frames for the operation of HPPs during weekdays and weekends are assumed, the electricity cost and revenue components in C_{1y} have two separate terms corresponding to different time frames in weekdays and weekends as follows:

$$\begin{aligned} C_{1y} = \sum_{i \in Z} \Big\{ & (P^{\omega_1}_{g_{iy}} \pi^{\omega_1}_{y} + P^{\omega_1}_{m_{iy}} \pi^{\omega_1}_{m_y} - P^{\omega_1}_{x_{iy}} \pi^{\omega_1}_{x_y}) \times h_{wd} \times 261 \\ & + (P^{\omega_2}_{g_{iy}} \pi^{\omega_2}_{y} + P^{\omega_2}_{m_{iy}} \pi^{\omega_2}_{m_y} - P^{\omega_2}_{x_{iy}} \pi^{\omega_2}_{x_y}) \times h_{we} \times 104 \Big\} \end{aligned} \tag{21}$$

3.2.2. Environmental Credit

C_{2y} represents the environmental credits assigned to FCVs in year y and can be stated as follows:

$$\begin{aligned} C_{2y} = \sum_{i \in Z} \Bigg\{ & FF_{iy}.\bar{\mu}_y.Nldv_{iy}.AM.SC_{CO_2}p.E_{CO_2} \\ & \times 10^{-3} \sum_{c \in VT} \left(\frac{VS_c}{FE_{gv_{cy}}} \right) \Bigg\} \end{aligned} \tag{22}$$

3.2.3. Emission Cost of Generation

C_{3y} represents the environmental costs of generation in year y, and similar to C_{1y}, has two terms corresponding to weekdays and weekends. Based on the mathematical formulation developed in Section 2, this cost component can be expressed as follows:

$$\begin{aligned} C_{3y} = \sum_{i \in Z} \Bigg\{ & \Big\{ ER_{chp_i} \left[V^{\omega_1}_{2_{iy}} - K^{\omega_1}_{2iy} \overline{P_{ga}}_{iy} + K^{\omega_1}_{3iy} \left(\overline{P_{gb}}_{iy} - \overline{P_{ga}}_{iy} \right) \right] \\ & + ER_{coal_i} \left(V^{\omega_1}_{3_{iy}} - K^{\omega_1}_{3iy} \overline{P_{gb}}_{iy} \right) \Big\} SC_{CO_2} g \times h_{wd} \times 261 \\ & + \Big\{ ER_{chp_i} \left[V^{\omega_2}_{2_{iy}} - K^{\omega_2}_{2iy} \overline{P_{ga}}_{iy} + K^{\omega_2}_{3iy} \left(\overline{P_{gb}}_{iy} - \overline{P_{ga}}_{iy} \right) \right] \\ & + ER_{coal_i} \left(V^{\omega_2}_{3_{iy}} - K^{\omega_2}_{3iy} \overline{P_{gb}}_{iy} \right) \Big\} SC_{CO_2} g \times h_{we} \times 104 \Bigg\} \end{aligned} \tag{23}$$

3.2.4. Hydrogen Transportation Cost

C_{4y} represents total hydrogen transportation costs, including the capital and operating costs of compressed gas trucks, which can be stated as follows:

$$C_{4y} = PC_y.CC_{cab}(1 - S_{cab_y}) + PT_y.CC_{tube}(1 - S_{tube_y}) + \sum_{(i,j)\in Z^*} 2OC_y.d_{ij}.N_{ijy} \times 365 \tag{24}$$

Based on straight-line depreciation, the salvage values for cab and tube trailers in (24) can be calculated as follows:

$$S_{cab_y}=\begin{cases} \frac{1}{(1+DR)^{(H-y+1)}}\left(\frac{y+LT_{cab}-H-1}{LT_{cab}}\right) & \forall y \geq H-LT_{cab} \\ 0 & \text{otherwise} \end{cases} \tag{25}$$

$$S_{tube_y}=\begin{cases} \frac{1}{(1+DR)^{(H-y+1)}}\left(\frac{y+LT_{tube}-H-1}{LT_{tube}}\right) & \forall y \geq H-LT_{tube} \\ 0 & \text{otherwise} \end{cases} \tag{26}$$

3.3. Constraints

3.3.1. Transmission System

Given the nature of the presented planning studies, which only require an approximate representation of the grid, a dc power flow model that accounts for the transmission system losses is adopted here [35]. Thus, the power losses in line (i, j) of the electricity network can be approximately calculated as:

$$Ploss_{ij} \cong g_{ij}(\delta_i - \delta_j)^2 \tag{27}$$

Following the method proposed in [36] with some modifications, a linear approximation of power losses in year y and during the time period of τ can be obtained using L piecewise linear blocks as follows:

$$\delta^{\tau}_{ijy} = \left|\delta^{\tau}_{iy} - \delta^{\tau}_{jy}\right| \tag{28}$$

$$\delta^{\tau}_{ijy} = \sum_{l=1}^{L} \delta^{\tau}_{ijy}(l) \tag{29}$$

$$Ploss^{\tau}_{ijy} = g_{ijy} \sum_{l=1}^{L} \alpha_{ijy}(l)\delta^{\tau}_{ijy}(l) \tag{30}$$

Assuming that each angle block has a constant maximum length $\Delta\delta_y$, the slope of the blocks of angles for all lines (i, j) can be calculated as:

$$\alpha_{ijy}(l) = (2l - 1)\Delta\delta_y \quad \forall(i, j) \in \Omega \wedge y \in Y \tag{31}$$

Consequently, each block of voltage angle is bounded between zero and $\Delta\delta_y$, as follows:

$$0 \leq \delta^{\tau}_{ijy}(l) \leq \Delta\delta_y \quad \forall(i, j) \in \Omega \wedge y \in Y \wedge \tau \in \Psi \wedge l \in L_1 \tag{32}$$

To linearize the absolute value in (28), two new nonnegative variables $\delta^{\tau+}_{ijy}$ and $\delta^{\tau-}_{ijy}$ are defined, together with the following constraints [37]:

$$\begin{gathered} \delta^{\tau}_{ijy} = \delta^{\tau+}_{ijy} + \delta^{\tau-}_{ijy} \\ \delta^{\tau}_{iy} - \delta^{\tau}_{jy} = \delta^{\tau+}_{ijy} - \delta^{\tau-}_{ijy} \\ \delta^{\tau+}_{ijy} \geq 0, \delta^{\tau-}_{ijy} \geq 0 \\ \forall(i, j) \in \Omega \wedge y \in Y \wedge \tau \in \Psi \end{gathered} \tag{33}$$

The following constraints are also needed to enforce the adjacency of the angle blocks:

$$\mu^{\tau}_{ijy}(l).\Delta\delta_y \leq \delta^{\tau}_{ijy}(l) \quad \forall(i,j) \in \Omega \wedge y \in Y \wedge \tau \in \Psi \wedge l \in L_2 \tag{34}$$

$$\delta^{\tau}_{ijy}(l) \leq \mu^{\tau}_{ijy}(l-1).\Delta\delta_y \quad \forall(i,j) \in \Omega \wedge y \in Y \wedge \tau \in \Psi \wedge l \in L_3 \tag{35}$$

$$\mu^{\tau}_{ijy}(l) \leq \mu^{\tau}_{ijy}(l-1) \quad \forall(i,j) \in \Omega \wedge y \in Y \wedge \tau \in \Psi \wedge l \in L_4 \tag{36}$$

Considering the line-loss model just described, the net power injected at zone i in year y and during the time period of τ can be represented as:

$$P^{\tau}_{iy} = \sum_{(i,j)\in\Omega} \left[\frac{1}{2} g_{ijy} \sum_{l=1}^{L} \alpha_{ijy}(l) \delta^{\tau}_{ijy}(l) - b_{ijy}(\delta^{\tau}_{iy} - \delta^{\tau}_{jy}) \right] \tag{37}$$

As a result, the zonal-power-balance constraints can be generally formulated as follows:

$$\begin{aligned} & P^{\tau}_{g_{iy}} - P^{\tau}_{l_{iy}} + P^{\tau}_{m_{iy}} - P^{\tau}_{x_{iy}} \\ & - \sum_{(i,j)\in\Omega} \left[\frac{1}{2} g_{ijy} \sum_{l=1}^{L} \alpha_{ijy}(l) \delta^{\tau}_{ijy}(l) - b_{ijy}(\delta^{\tau}_{iy} - \delta^{\tau}_{jy}) \right] = 0 \\ & \forall i \in Z \wedge y \in Y \wedge \tau \in \Psi \end{aligned} \tag{38}$$

where the total base load in each zone (P_l) is comprised of the zonal electricity demand (P_e) and the total installed HPPs as follows:

$$P^{\tau}_{l_{iy}} - P^{\tau}_{e_{iy}} - P_{hpp_{iy}} = 0 \quad \forall i \in Z \wedge y \in Y \wedge \tau \in \Psi \tag{39}$$

3.3.2. Transmission Capacity Constraints

Based on the transmission model discussed in the previous section, these constraints can be defined as follows:

$$\begin{aligned} -b_{ijy}(\delta^{\tau}_{iy} - \delta^{\tau}_{jy}) + \frac{1}{2} g_{ijy} \sum_{l=1}^{L} \alpha_{ijy}(l) \delta^{\tau}_{ijy}(l) \leq \overline{Pd}_{ijy} \\ b_{ijy}(\delta^{\tau}_{iy} - \delta^{\tau}_{jy}) + \frac{1}{2} g_{ijy} \sum_{l=1}^{L} \alpha_{ijy}(l) \delta^{\tau}_{ijy}(l) \leq \overline{Pr}_{ijy} \\ \forall(i,j) \in \Omega \wedge y \in Y \wedge \tau \in \Psi \end{aligned} \tag{40}$$

The maximum limits $\overline{Pd}_{ijy}$ and $\overline{Pr}_{ijy}$ are obtained based on thermal and stability considerations.

3.3.3. Zonal Power Generation Limits

These limits are the minimum and maximum effective generation capacities (including the capacity factors) which are available in each zone during the planning years in the time period of τ:

$$\underline{P_g}_{iy} \leq P^{\tau}_{g_{iy}} \leq \overline{P_g}_{iy} \quad \forall i \in Z \wedge y \in Y \wedge \tau \in \Psi \tag{41}$$

The lower bounds $\underline{P_g}_{iy}$ may be set based on the operational considerations of the base-load generation resources in each zone.

3.3.4. Zonal Import/Export Power Limits

These limits can be stated as:

$$\begin{gathered}\underline{P_{m}}_{iy} \leq P_{m}^{\tau}{}_{iy} \leq \overline{P_{m}}_{iy} \\ \underline{P_{x}}_{iy} \leq P_{x}^{\tau}{}_{iy} \leq \overline{P_{x}}_{iy} \\ \forall i \in Z \wedge y \in Y \wedge \tau \in \Psi\end{gathered} \tag{42}$$

3.3.5. HPP Placement Constraints

As per the notation used in Section 3.1, these constraints are represented by:

$$\begin{gathered}0 \leq P_{hpp_{iy}} \leq \overline{P_{hpp}}_{iy} \\ 0 \leq \Delta P_{hpp_{iy}} \leq \overline{\Delta P_{hpp}}_{iy} \\ \overline{P_{hpp}}_{iy_1} = 0 \\ \forall i \in Z \wedge y \in Y_1\end{gathered} \tag{43}$$

where $\overline{P_{hpp}}_{iy}$ is the maximum size of HPPs, which is allowed to be installed in zone i by year y, and $\overline{\Delta P_{hpp}}_{iy}$ is the maximum annual development of HPPs in zone i. $\overline{P_{hpp}}_{iy}$ is equal to zero for the first year of the planning horizon.

3.3.6. Hydrogen Transportation Constraints

As discussed in Section 3.1, hydrogen transportation constraints can be expressed by (7) and (11)–(19).

3.3.7. Generation Emission Constraints

Based on the model developed in Section 2, these constraints can be expressed by (4) and (5).

3.3.8. Penetration Constraints

These constraints can be defined as follows:

$$0 \leq FF_{iy} \leq 1 \quad \forall i \in Z \wedge y \in Y \tag{44}$$

$$FF_{iy}\overline{\mu}_{y} - FF_{iy-1}\overline{\mu}_{y-1} \geq 0 \quad \forall i \in Z \wedge y \in Y_1 \tag{45}$$

where (44) state that the penetration levels in each year cannot exceed the limits $\overline{\mu}_{y}$ set by the assumed transition curve, and (45) enforce the increase of the ultimate penetration levels over time, so that the total number of FCVs in the transport sector in each year cannot be less than in a previous year. Furthermore, the following constraints should be considered in the model for a uniform hydrogen economy penetration in all zones:

$$FF_{iy} - FF_{jy} = 0 \quad \forall i, j \in Z \wedge y \in Y_1 \tag{46}$$

4. Data Uncertainty & Robust Optimization

Optimization models such as the one previously developed often rely on input parameters whose values must be estimated. The estimated parameter values, however, may be different from the true values; this disparity might be due to data limitations, biased data, unrealistic assumptions, numerical errors in the estimation process or the nonstationary nature of the data. On the other hand, errors in estimating input parameters may severely affect the obtained optimal solution and its actual performance. Thus, as the data take values different than nominal or expected ones, several constraints may be violated, and the optimal solution yielded by the nominal data may no longer be optimal or even feasible. Therefore, due to the impact of data uncertainty on the quality and feasibility of the optimization models, methodologies should be adopted that appropriately deal with the uncertainty of the parameters in the model [38, 39].

Sensitivity analysis and stochastic programming are the classical approaches for dealing with parameter uncertainty in optimization models [40]–[43]. Sensitivity analyses such as Monte Carlo simulations [44], which are used in this work, measure the sensitivity of a solution to stochastic changes in the input parameters; however, it provides no mechanism by which this sensitivity can be controlled. In this regard, it can be counted as a reactive approach to deal with uncertainty [41]. In the stochastic programming approach, it is assumed that the probability distributions of the uncertain input parameters are known or can be estimated with reasonable accuracy. The goal in this approach is to find a solution that is feasible for all (or almost all) possible instances of the data and to maximize the expectation of some function of the decision and the random variables. For example, in chance constrained stochastic programming models where the feasibility of a solution is expressed by chance constraints, a feasible solution is not required to satisfy every outcome of the random parameters, but it is required to be feasible with at least some specified probability [45]. There are inherent difficulties with this approach: First, while the optimal decision variables can be quite sensitive to the distributions of the random parameters, it is difficult, in practice, to accurately estimate these distributions; therefore, the obtained solution can be considered as only an approximation. Second, even if the distributions are known, it is still computationally difficult to evaluate the chance constraints. Finally, the convexity of the model can be lost due to the introduction of chance constraints which increases the complexity of the original optimization model [46, 47].

One of the alternative approaches to optimization under uncertainty, which has attracted significant attention over the last decade, is *robust optimization* [48, 49]. In classic robust optimization, parameter uncertainty is defined by an uncertainty set which includes all or most possible realizations of the data. Given an uncertainty set for uncertain input parameters, robust optimization seeks for an uncertainty-immunized solution which remains feasible in all realizations of the input data, and the value of the objective function at this solution has the best worst performance over all of the feasible solutions. To obtain a robust optimal solution one first needs to transform the two-layer optimization problem into a deterministic one-layer problem. This one-layer deterministic problem is called the *robust counterpart problem*. Given the nonempty uncertainty sets, to obtain a robust optimal solution which optimizes the worst-case performance when the input data belong to the uncertainty sets, the following problem is solved:

$$\begin{aligned} \min \quad & \max \quad f_0(\boldsymbol{x}, \boldsymbol{d}_0) \\ \text{s.t.} \quad & f_e(\boldsymbol{x}, \boldsymbol{d}_e) \geq 0 \quad \forall e \in E, \forall \boldsymbol{d}_e \in U_e \end{aligned} \tag{47}$$

where for $e \in E \cup \{0\}$, the set U_e is the nonempty uncertainty set of the parameter $\boldsymbol{d}_e$. Although this approach provides immunization to parameter uncertainty, its results are perceived to be too conservative for real applications, i.e., robustness is ensured at the cost of significantly losing optimality [39, 46]. To rectify this shortcoming of robust optimization, it has been suggested in the literature (e.g., [50]–[54]) to intelligently shrink the uncertainty set. One of such techniques was proposed in [38], which is also applicable to discrete optimization models [55]. The main feature of this formulation is that it does not involve solving a nonlinear problem; therefore, the tractability of the problem is not affected. Furthermore, in this approach, conservativeness of the approach can be controlled. In this paper, this approach is adopted to develop the robust optimization model for transition to FCVs that is briefly explained next [38, 39, 55].

Consider the following general linear programming model:

$$\begin{aligned} \min \quad & \mathbf{c}'\mathbf{x} \\ \text{s.t.} \quad & \tilde{\mathbf{a}}_e'\mathbf{x} \geq b_e \quad \forall e \\ & \mathbf{x} \in X \end{aligned} \tag{48}$$

where X includes all mixed integer feasible solutions. Without loss of generality, it is assumed that uncertainty only affects the constraint coefficients $\tilde{\mathbf{a}}_e$, since even problems with uncertainty in the cost vector $\mathbf{c}$ and the right-hand side b_e can be reformulated so that all uncertainties only appear in $\tilde{\mathbf{a}}_e$. Thus, problem

(48) can be rewritten as follows:

$$\begin{aligned} \min \ & W \\ \text{s.t.} \ & W - \mathbf{c}'\mathbf{x} \geq 0 \\ & \tilde{\mathbf{a}}_e'\mathbf{x} \geq b_e \ \ \forall e \\ & \mathbf{x} \in X \end{aligned} \tag{49}$$

in which uncertainty in the objective function has been transferred to the constraints. It is assumed that every element of the vector $\tilde{\mathbf{a}}_e$, i.e., $\tilde{a}_{ev}$, $v \in \{1, 2, ..., n\}$, is subject to uncertainty and belongs to a symmetrical interval $[\hat{a}_{ev} - \Delta a_{ev}, \hat{a}_{ev} + \Delta a_{ev}]$ known by the decision-maker, where $\hat{}$ and Δ are used to represent nominal values and deviation magnitudes, respectively. This interval is centered at the point forecast $\hat{a}_{ev}$, while Δa_{ev} measures the precision of the estimate. The scaled deviation s_{ev} of parameter $\tilde{a}_{ev}$ from its nominal value can then be defined as:

$$s_{ev} = \frac{\tilde{a}_{ev} - \hat{a}_{ev}}{\Delta a_{ev}} \tag{50}$$

which belongs to [-1,1]. The aggregate scaled deviation for constraint e, $\sum_{v=1}^{n} |s_{ev}|$, which is more accurate than individual ones, can take any value between 0 and n; however, it is unlikely that all of the coefficients $\tilde{a}_{ev}$ take their worst cases simultaneously [55]. Consequently the true value of $\sum_{v=1}^{n} |s_{ev}|$ can be assumed to be in a narrower range. This point is expressed in mathematical terms as follows:

$$\sum_{v=1}^{n} |s_{ev}| \leq \Gamma_e \ \ \forall e \tag{51}$$

The parameter $\Gamma_e \in [0, n]$, called the *budget of uncertainty* of constraint e, adjusts the robustness against the level of conservatism of the solution. The value of this parameter reflects the attitude of the decision-maker toward uncertainty. When $\Gamma_e = 0$, there is no "protection" against uncertainty; on the other hand, $\Gamma_e = n$ yields a very conservative solution, since this can be interpreted as all the uncertain parameters' taking their worst-case values at the same time. For any values between 0 and n, the decision-maker makes a trade-off between the protection level of the constraint and the degree of conservatism of the solution. In this context, the uncertainty set U_e becomes:

$$U_e = \{(\tilde{a}_{ev}) \mid \tilde{a}_{ev} = \hat{a}_{ev} + \Delta a_{ev} s_{ev}, \forall e, v, s_{ev} \in S_e\} \tag{52}$$

where:

$$S_e = \left\{ \mathbf{s}_e = [s_{e1}, s_{e2}, ..., s_{en}] \mid |s_{ev}| \leq 1, \forall v, \sum_{v=1}^{n} |s_{ev}| \leq \Gamma_e \right\} \tag{53}$$

A robust optimal solution can then be obtained from the following counterpart problem:

$$\begin{aligned} \min \ & \mathbf{c}'\mathbf{x} \\ \text{s.t.} \ & \hat{\mathbf{a}}_e'\mathbf{x} + \min_{\mathbf{s}_e \in S_e} \sum_{v=1}^{n} \Delta a_{ev} x_v s_{ev} \geq b_e \ \ \forall e \\ & \mathbf{x} \in X \end{aligned} \tag{54}$$

By applying strong duality, based on Theorem 1 in [38], (54) can be shown to be equivalent to the following

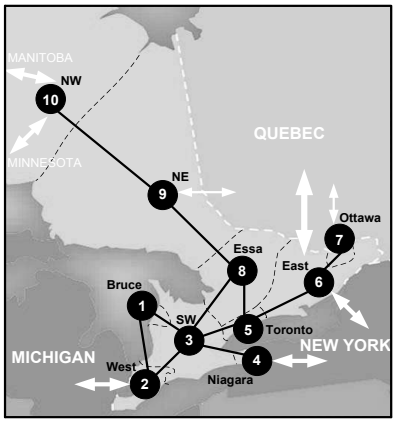

Figure 5: Simplified model of Ontario's grid.

problem, which is a linear programming model:

$$
\begin{aligned}
\min \quad & \mathbf{c}'\mathbf{x} & & \\
\text{s.t.} \quad & \hat{\mathbf{a}}_e'\mathbf{x} - \Gamma_e p_e - \sum_{v \in V_e} q_{ev} \geq b_e & & \forall e \in E \\
& p_e + q_{ev} \geq \Delta a_{ev} r_v & & \forall e \in E \wedge v \in V_e \\
& -r_v \leq x_v \leq r_v & & \forall v \in V \\
& p_e \geq 0 & & \forall e \in E \\
& q_{ev} \geq 0 & & \forall e \in E \wedge v \in V_e \\
& r_v \geq 0 & & \forall v \in V \\
& \mathbf{x} \in X & & (55)
\end{aligned}
$$

Note that this robust formulation requires the determination of a budget of uncertainty $\Gamma_e \in [0, |V_e|]$ for each constraint e subject to uncertainty, as well as the definition of new decision variables p_e, q_{ev} and r_v.

It can be shown that the robust solution will remain feasible with a high probability even when more than a specified number of uncertain coefficients changes. It has, in fact, been verified that for constraint e with n uncertain parameters to be violated with the probability of at most ε_e, a budget of uncertainty Γ_e at least equal to $1 + \Phi^{-1}(1 - \varepsilon_e)\sqrt{n}$ is adequate, where Φ is the cumulative distribution of a standard normal [38]. The violation probability of constraint e being given a budget of uncertainty Γ_e can also be calculated from $1 - \Phi\left(\frac{\Gamma_e - 1}{\sqrt{n}}\right)$.

5. Application to Ontario, Canada

This section discusses the application of the proposed optimization model to the real-case example of Ontario, Canada, considering the issue of data uncertainty. Ontario's Independent Electricity System Operator (IESO) represents the Ontario network with ten zones servicing more than 12 million people [56]. This same representation is used in this study to develop the 10-bus simplified model of Ontario's network, as shown in Fig. 5, which considers the main grid load and generation centers and transmission corridors. This model is mostly a 500 kV network, with a 230 kV interconnection between Northeast (NE) and Northwest (NW).

5.1. Economic Assessment

According to Ontario's IESO, on-peak hours are defined as hours 8 to 23 Monday to Friday with the total of 5×16 hours per week; Hour 8 is 7:00-8:00 and Hour 23 is 22:00-23:00. All remaining hours as well

as holidays are defined as off-peak. This gives an indication of the operation time periods when the HPPs could take advantage of the low electricity price and demand in the system. Hence, this study assumes an 8 weekday and 14 weekend off-peak hours; this results in 68 hours operation per week or almost a 40% capacity factor.

The economic viability of electrolytic hydrogen production during off-peak hours is investigated here, considering the typical electricity market prices in Ontario. Thus, a literature survey was performed regarding the investment costs for different components of a hydrogen production unit, considering size and economies of scale [9, 69, 70, 71],[57]–[68]. A 300 kW hydrogen production unit is assumed in this study; this is the installed power of a unit including a rectifier, electrolyzer and compressor with an overall efficiency of 70%. Based on HHV of hydrogen (39.45 kWh/kg), the hydrogen production rate of this unit is found to be equal to 5.32 kg/h (59.31 Nm^3/h). As per [72], the energy requirement of a multi-stage compressor for the compression of hydrogen up to 400 bar is equal to almost 9% of its HHV. Based on the maximum flow rate of 5.32 kg/h, the maximum demanding power of the multi-stage compressor is found to be equal to almost 19 kW; this tranlates to almost 3.5 kW per kg/h hydrogen flow at high pressure. Consequently, the maximum installed power of the electrolyzer would be equal to 281 kW. The assumed investment cost of an electrolyzer is 65,000 CAD per kg/h hydrogen including electrolyzer stack, gas and water conditioning, power electronics and control systems. The hydrogen storage at 400 bar is sized to hold the average one-day hydrogen production, and its investment cost is assumed to be 600 CAD/kg. The total investment cost of hydrogen storage is found based on the assumed operation hours during weekdays and weekends. The investment cost of multi-stage compressor is assumed to be 2,500 CAD/kW or alternatively 8,876 CAD per kg/h of hydrogen. Also, 10% of the total initial investment for the whole unit is assumed to cover the average annual operation and maintenance costs; these costs include labour, insurance, property tax, licensing, maintenance and repair [8, 67].

Despite a general decline in off-peak electricity prices in Ontario [33], the average HOEP in the first year of the planning horizon both on weekdays and weekends, i.e., 31.72 and 34.91 CAD/MWh, respectively, are assumed as the expected electricity prices during the lifetime of the plant. Based on these electricity prices and typical discount rates of 8% and a plant lifetime of 20 years (because of low capacity factor), and disregarding the income tax as well as any government support program, the minimum hydrogen selling price to justify the investment is found to be equal to 6.40 CAD/kg. Thus, this price makes the net present value greater than zero, and yields an 8% internal rate of return and a profitability index greater than unity. This price can be approximately compared to a gasoline price of 1 CAD/liter, assuming the fuel economies of FCVs and ICEs to be 100 km/kg and 11.5 km/liter, respectively, and the cost of hydrogen delivery and dispensing to be 2.5 CAD/kg [34]. This analysis demonstrates the feasibility of electrolytic hydrogen production during off-peak hours for Ontario's transport sector, even disregarding the environmental benefit of producing hydrogen through electrolysis versus other more polluting mechanisms such as steam reforming of natural gas. It should also be emphasized that this analysis has made a conservative assumption by considering that the grid is constrained with respect to transmission and generation during the peak demand hours of the day, thus assuming that hydrogen for the transport sector can only be produced during off-peak hours.

5.2. Sensitivity Analysis

The optimization model for planning the transition to FCVs in Ontario, Canada involves many parameters with inherent estimation errors. A common approach to investigate the impact of estimation errors on the optimal solution and the corresponding optimal value is to represent the errors as perturbations to the data in order to perform a sensitivity analysis on the optimal solution [73]. The results of this sensitivity analysis reveal the most influential uncertain parameters on the optimal value that can later be used for developing the robust counterpart problems.

The required sensitivity analysis is carried out here based on Monte Carlo simulation. This yields the impact of estimation errors in the parameters of the model developed in Section 3. More precisely, given a parameter A in an optimization problem, M perturbations ΔA are generated to represent the estimation errors in the parameter A. Here, it is assumed that the perturbations have independent normal distributions,

i.e.,

$$\Delta A = \rho \lambda A \tag{56}$$

where parameter $\rho \in (0, 1]$ indicates the size of the relative perturbation and λ is a random parameter, which is assumed to follow a normal distribution with zero mean and unit standard deviation. Here, ρ and M are fixed at 10% and 1000, respectively; these values were chosen considering a reasonable perturbation level of 10%, and 1000 perturbations since satisfactory results are obtained from Monte Carlo simulations for this number (increasing the number of Monte Carlo simulations beyond 1000 did not yield any significant changes to the final solutions). It is also assumed that only one parameter of the optimization model is perturbed at a time while all other parameters remain at their nominal or expected values.

In this sensitivity analysis, the following three quantities are considered and distinguished [74, 75]:

1. *True optimal value*: It is the value of the objective function (OF) using an unperturbed parameter A at the optimal solution obtained from the unperturbed parameter A; this is denoted by $OF_A(X_A)$.
2. *Actual optimal value*: It is the value of the objective function using an unperturbed parameter A at the optimal solution obtained from the perturbed parameter $A + \Delta A$; this is denoted by $OF_A(X_{A+\Delta A})$.
3. *Estimated optimal value*: It is the value of the objective function using a perturbed parameter $A + \Delta A$ at the optimal solution obtained from the perturbed parameter $A + \Delta A$; this is denoted by $OF_{A+\Delta A}(X_{A+\Delta A})$.

In practice, unperturbed or true values of the parameters are unknown to the decision maker at the time of planning; therefore, an optimal solution is obtained from the perturbed or estimated parameters $A + \Delta A$, which are the only available data. During the simulation process, some typical values of the parameters are chosen to represent true values; these assumed true values A are then used to generate perturbations ΔA and to obtain $A + \Delta A$, which represent the estimated value of the parameters. An optimal solution is then found at the estimated parameters, denoted by $X_{A+\Delta A}$. This optimal solution along with the true value of the parameter A, is used to calculate the actual optimal value $OF_A(X_{A+\Delta A})$. This actual optimal value determines the performance of the decision made using the estimated data which is the quantity of interest. Note that the estimated optimal value, i.e., $OF_{A+\Delta A}(X_{A+\Delta A})$ might underestimate or overestimate the objective function value and, therefore, is not useful for planning studies.

It should be mentioned that typical methods used in the literature for sensitivity analysis are valid for small perturbations, allowing to approximately determine the *estimated* optimal value [76, 77]. However, these methods would not be appropriate here to obtain the *actual* optimal value given the larger range of parameter variation considered.

In order to quantitatively compare the sensitivity of the optimal value to perturbations of different parameters, the following *Average Deviation Index (ADI)* measure is proposed:

$$ADI = \frac{1}{M} \sum_{m=1}^{M} \left| OF_A(X_{A+\Delta A_m}) - OF_A(X_A) \right| \tag{57}$$

where $OF_A(X_{A+\Delta A_m})$ is the actual optimal value in simulation m. Calculated ADI values for different parameters in each optimization model are ranked to identify the most influential parameters, which are used later in developing the robust counterpart optimization model. The detailed implementation of this method for the previously developed optimization model is presented next.

In performing a sensitivity analysis using Monte Carlo simulation of the optimization model for the transition to a hydrogen economy, the following assumptions are made:

- *Number of parameters*: In total, 23 single or group parameters are considered which cover the most relevant parameters involved in this optimization model.
- *Type of penetration and transition*: In order to impose a more limiting condition on the electricity grid and the hydrogen transportation network, a uniform penetration of FCVs in different zones following Transition curve 2 in Fig. 4 is assumed.

Table 1: Optimal uniform FCV penetration in Ontario, Canada for different values of emission costs

Emission cost [CAD/ton]	10	50	75	100	110	125	150	175	200	250	300	400	500	700
FCV penetration [%]	0	0	0	0.06	2.90	2.95	3.02	3.29	3.38	3.79	4.13	4.41	4.43	4.43

- *Hydrogen-related constraints*: To include more realistic development and operational limits, a 20 MW HPP placement constraint and a 4 ton/day limit (equal to 10 compressed gas trucks) for transporting hydrogen in each route are considered.
- *Emission constraints for generation*: These are disregarded here because they make the optimization problem much harder to solve, which is certainly an issue when thousands of simulations are required in Monte Carlo simulation approach. However, these constraints are considered in the robust optimization analyses.
- *Social cost of emissions*: With regard to typical electricity prices in Ontario, emission costs lower than 125 CAD/ton substantially reduces the potential penetration levels obtained from solving the deterministic optimization model described in Section 3, as shown in Table 1. Although typical values used for this parameter in the literature for CO_2 emissions are somewhat less than 125 CAD/ton, this value was chosen due to the fact that the environmental benefits of FCVs are not merely limited to the reduction of CO_2 emissions as per the discussions in Section 2. It is important to highlight that those parameters whose estimation errors are not expected to be larger than 10% are included in the list of uncertain parameters for performing sensitivity analysis or developing the robust models. Since the reported values of the social cost of emissions vary in an extremely wide range and are really unknown in practice, as there is currently no mechanism to precisely price emissions, this parameter is treated here differently from other uncertain parameters; therefore emission costs are not placed in the same category of the other uncertain parameters analyzed in this study. Furthermore, note that the 4.4% maximum potential penetration of FCVs in Table 1 translates to 379,781 FCVs. In order to achieve this, at most 94 trucks are required in each individual year of the planning horizon. Although the daily mileage of these trucks is more than that of LDVs, the corresponding total mileage compared to the total mileage of LDVs is negligible; thus, the CO_2 emission costs of trucks are not considered in these studies.

The readers are referred to [33] for further details regarding the Ontario's electricity and transport sectors data.

For the sensitivity analysis, the AMPL [78] modeling language with a CPLEX [79] solver were used on an IBM eServer xSeries 460 with 8 Intel Xeon 2.8 GHz processors and 3 GB (effective) of RAM, to perform the Monte Carlo simulations and determine the true and actual optimal values; other computational tasks were performed using MATLAB [80]. Also, in order to achieve a high degree of precision, optimality gap was fixed at 0.02% for all the simulations. The calculated ADI values, together with the ranking of the parameters, are reflected in Table 2. Based on the presented results, annual mileage and fuel economy of fuel cell vehicles are found to be the most influential parameters in this sensitivity analysis. However, hydrogen transfer related parameters have no impact on the optimal solution. This result is expected, since with the chosen value of the social cost of CO_2 emission, hydrogen economy penetration levels are relatively low, which, in turn, requires less hydrogen to be transported between the zones. Also, internal electricity prices in Ontario as well as import and export electricity prices are found to have an average-to-high impact on the optimal solution. Based on these observations and as shown in Table 2, all the involved parameters in the optimization model for the transition to hydrogen economy can be classified into three categories based on their relative impact on the optimal solution.

As highlighted in the list of assumptions for the sensitivity analysis, an average 10% deviation for all the parameters is considered. However, given the limitation of the robust optimization techniques including the one used here, uncertain parameters such as annual mileage and fuel economy of FCVs which simultaneously

Table 2: Average deviation index of the FCV transition model for different uncertain parameters.

Rank	Uncertain parameter	ADI [CAD]
1	Annual mileage	3.4605e+007
2	Fuel economy of FCVs	3.3263e+007
3	HOEP on weekdays	5.7007e+006
4	Price of export power on weekdays	5.5155e+006
5	HOEP on weekends	4.7217e+006
6	Price of export power on weekends	4.5095e+006
7	Price of import power on weekdays	4.0228e+006
8	Price of import power on weekends	3.2643e+006
9	Average fuel economy of GVs	2.7609e+006
10	Annual growth rate of LDVs in Toronto	2.0736e+006
11	Efficiency improvement of HPPs	1.8587e+006
12	Annual growth rate of LDVs in SW	7.7110e+005
13	Annual growth rate of LDVs in Ottawa	4.5828e+005
14	Annual growth rate of LDVs in West	3.7876e+005
15	Annual growth rate of LDVs in Essa	3.2004e+005
16	Annual growth rate of LDVs in East	2.1949e+005
17	Annual growth rate of LDVs in NE	1.6075e+005
18	Annual growth rate of LDVs in Niagara	4.8479e+004
19	Annual growth rate of LDVs in Bruce	5.9460e+003
20	Annual growth rate of LDVs in NW	3.7698e+003
21	Average operating cost of hydrogen transfer	0
22	Capital cost of tube trailer	0
23	Capital cost of cab	0

appear in multiple constraints and the objective function cannot be handled by this methodology, hence, to be conservative, the worst-case values of these parameters were used for the robust optimization studies. The most-appealing decision variable in the proposed optimization model for transition to FCVs is the feasibility factor (FF_{iy}), since it translates into penetration levels ($\bar{\mu}_y FF_{iy}$) or total number of FCVs by the end of the planning horizon. To determine the worst-case values for these two parameters, an analysis of their effects on total number of FCVs was performed. From this study, the worst-case value for fuel economy of FCVs is found to be 90% of its nominal or expected value, while the worst-case value of the annual mileage corresponds to 110% of its nominal value. Observe that the other uncertain parameters are basically electricity prices and fuel economy of GVs which only appear on the objective function and can then be studied using the robust optimization method discussed in Section 4.

5.3. Robust Model for Transition to FCVs

This section presents the robust optimization model for the transition to FCVs that is robust with respect to uncertainty in the parameters identified in the previous section. This model is based on the method discussed in Section 4, which is capable of adjusting the degree of conservatism, as explained in detail next.

For the three sets of electricity prices (internal, import, and export), two time periods (ω_1 and ω_2), one set of fuel economy values for GVs and a planning span of 18 years, (49) presents 126 uncertain parameters

as follows:

$$0.9\widehat{\pi}_y^\tau \le \widetilde{\pi}_y^\tau \le 1.1\widehat{\pi}_y^\tau,\ \Delta\pi_y^\tau = 0.1\widehat{\pi}_y^\tau, \quad \forall y \in Y \wedge \tau \in \Psi \tag{58}$$

$$0.9\widehat{\pi}_{m_y}^\tau \le \widetilde{\pi}_{m_y}^\tau \le 1.1\widehat{\pi}_{m_y}^\tau,\ \Delta\pi_{m_y}^\tau = 0.1\widehat{\pi}_{m_y}^\tau, \quad \forall y \in Y \wedge \tau \in \Psi \tag{59}$$

$$0.9\widehat{\pi}_{x_y}^\tau \le \widetilde{\pi}_{x_y}^\tau \le 1.1\widehat{\pi}_{x_y}^\tau,\ \Delta\pi_{x_y}^\tau = 0.1\widehat{\pi}_{x_y}^\tau, \quad \forall y \in Y \wedge \tau \in \Psi \tag{60}$$

$$0.9\widehat{FEgv_y} \le \widetilde{FEgv_y} \le 1.1\widehat{FEgv_y}, \Delta FEgv_y = 0.1\widehat{FEgv_y}, \quad \forall y \in Y \tag{61}$$

Note that in the FCV transition model, disregarding the different types of LDVs, it is assumed that the FCV is replaced by a representative gasoline-powered vehicle with an average fuel economy of $FEgv_y$. By defining $EFgv_y = 1/FEgv_y$, the constraints in (61) can be represented as follows:

$$\frac{1}{1.1\widehat{FEgv_y}} \le \widetilde{EFgv_y} \le \frac{1}{0.9\widehat{FEgv_y}}, \Delta EFgv_y \simeq \frac{0.1}{\widehat{FEgv_y}}, \quad \forall y \in Y \tag{62}$$

so that (22) is linear with regard to this parameter. Therefore, in (55), $E = \{1\}$ and $V_1 = V = \{1, ..., 126\}$, as all the 126 uncertain parameters are in a single constraint. Hence, the following constraints should be added to the constraints of the optimization model for transition to FCVs in Section 3.3:

$$W - \sum_{y \in Y} \frac{1}{(1+DR)^{y-y_1}} \left(C_{1y} - C_{2y} + C_{3y} + C_{4y}\right) - \Gamma_1 p_1 - \sum_{v \in V} q_{1v} \ge 0 \tag{63}$$

$$p_1 + q_{1v} \ge \Delta a_{1v} r_v \quad \forall v \in V = V_1 = \{1, ..., 126\} \tag{64}$$

where the deviations of the uncertain parameters are determined to be as follows:

$$\Delta a_{1v} = \begin{cases} \frac{8\times261}{(1+DR)^{v-1}} \Delta\pi_{y_1+v-1}^{\omega_1} & \forall v \in \{1, ..., 18\} \\ \frac{14\times104}{(1+DR)^{v-19}} \Delta\pi_{y_1+v-19}^{\omega_2} & \forall v \in \{19, ..., 36\} \\ \frac{8\times261}{(1+DR)^{v-37}} \Delta\pi_{m_{y_1+v-37}}^{\omega_1} & \forall v \in \{37, ..., 54\} \\ \frac{14\times104}{(1+DR)^{v-55}} \Delta\pi_{m_{y_1+v-55}}^{\omega_2} & \forall v \in \{55, ..., 72\} \\ \frac{8\times261}{(1+DR)^{v-73}} \Delta\pi_{x_{y_1+v-73}}^{\omega_1} & \forall v \in \{73, ..., 90\} \\ \frac{14\times104}{(1+DR)^{v-91}} \Delta\pi_{x_{y_1+v-91}}^{\omega_2} & \forall v \in \{91, ..., 108\} \\ \frac{\bar{\mu}_{y_1+v-109}.AM.SC_{CO_2}p.E_{CO_2}\times10^{-3}}{(1+DR)^{v-109}} \times \Delta EFgv_{y_1+v-109} & \forall v \in \{109, ..., 126\} \end{cases}$$

$$-r_v \le \sum_{i \in Z} P_{g_{i,y_1+v-1}}^{\omega_1} \le r_v \quad \forall v \in \{1, ..., 18\} \tag{65}$$

$$-r_v \leq \sum_{i \in Z} P^{\omega_2}_{g_{i,y_1+v-19}} \leq r_v \quad \forall v \in \{19, ..., 36\} \tag{66}$$

$$-r_v \leq \sum_{i \in Z} P^{\omega_1}_{m_{i,y_1+v-37}} \leq r_v \quad \forall v \in \{37, ..., 54\} \tag{67}$$

$$-r_v \leq \sum_{i \in Z} P^{\omega_2}_{m_{i,y_1+v-55}} \leq r_v, \quad \forall v \in \{55, ..., 72\} \tag{68}$$

$$-r_v \leq \sum_{i \in Z} P^{\omega_1}_{x_{i,y_1+v-73}} \leq r_v \quad \forall v \in \{73, ..., 90\} \tag{69}$$

$$-r_v \leq \sum_{i \in Z} P^{\omega_2}_{x_{i,y_1+v-91}} \leq r_v \quad \forall v \in \{91, ..., 108\} \tag{70}$$

$$-r_v \leq \sum_{i \in Z} (Nldv_{i,y_1+v-109}.FF_{i,y_1+v-109}) \leq r_v \quad \forall v \in \{109, ..., 126\} \tag{71}$$

where C_{1y} and C_{2y}, which include the main uncertain parameters are defined as follows, and C_{3y} and C_{4y} are the same as the ones previously represented by (23) and (24), respectively:

$$C_{1y} = \sum_{i \in Z} \Big\{ (P^{\omega_1}_{g_{iy}} \widehat{\pi}^{\omega_1}_{y} + P^{\omega_1}_{m_{iy}} \widehat{\pi}^{\omega_1}_{m_y} - P^{\omega_1}_{x_{iy}} \widehat{\pi}^{\omega_1}_{x_y}) \times 8 \times 261 + (P^{\omega_2}_{g_{iy}} \widehat{\pi}^{\omega_2}_{y} + P^{\omega_2}_{m_{iy}} \widehat{\pi}^{\omega_2}_{m_y} - P^{\omega_2}_{x_{iy}} \widehat{\pi}^{\omega_2}_{x_y}) \times 14 \times 104 \Big\} \tag{72}$$

$$C_{2y} = \sum_{i \in Z} \Big(FF_{iy}.\bar{\mu}_y.Nldv_{iy}.AM.SC_{CO_2}p.E_{CO_2}.\widehat{EF}gv_y \times 10^{-3} \Big) \tag{73}$$

5.4. Results and Discussion

The robust model developed for the transition to FCVs was formulated and solved with the same tools and settings used for the sensitivity analysis. This section presents and discusses the numerical results obtained using the same assumptions made for the sensitivity analysis in Section 5.2. Based on the discussions presented in Section 2, for the assumed social cost of emissions of 125 CAD/ton in the higher density population area, the corresponding emission cost of generation is assumed to be 10 CAD/ton; this value is used in the emission constraints for generation in the models. Note that in this case there is no need to neglect emission constraints for generation due to computational restrictions as in the case of Monte Carlo simulation analysis; this allows to analyze the effect of emission constraints for generation in the robust optimization results as shown next.

There is a direct impact on the optimal robust solution whenever there is an increase in the budget of uncertainty or protection level of the constraint with uncertain parameters. This is illustrated in Fig. 6, which demonstrates how optimality is affected with the increase of the budget of uncertainty. Figure 7 also depicts the trade-off between optimality and robustness; as anticipated, the higher probabilities of constraint violation coincide with lower losses of optimality (e.g., for an 8% loss of optimality, there is less than 1% probability of constraint violation when the emission constraints for generation are considered). It is also interesting to note that the impact of emission constraints for generation is more significant for lower violation probabilities. Note as well that when the violation probability is lower than, for instance, 5%, the loss of optimality is slightly less if emission constraints for generation are considered.

Samples of the objective function values and the probability bounds of constraint violation are presented in Table 3. Observe that under zero ($\Gamma = 0$) and under full protection ($\Gamma = 126$) of the constraint with uncertain parameters, the optimal value is increased by 0.21% and 10.42%, respectively; hence, reducing

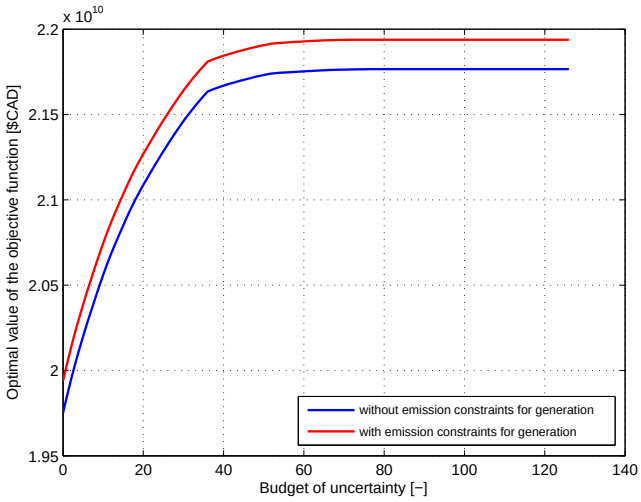

Figure 6: Impact of the budget of uncertainty Γ on the optimal value of the robust FCV transition model.

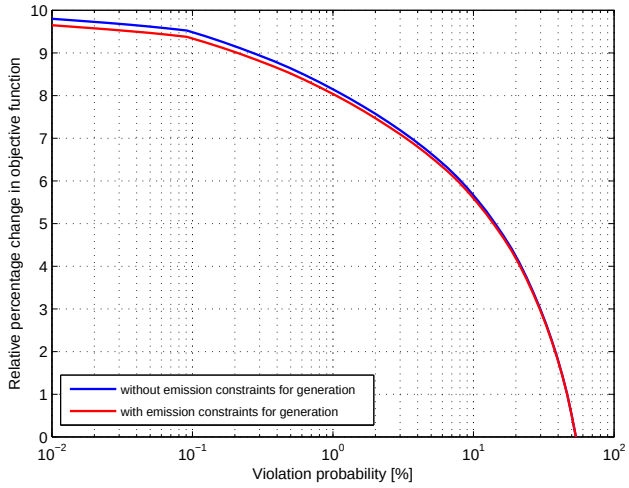

Figure 7: Relative change in optimal value of the robust FCV transition model with respect to the probability bound of constraint violation.

the chance of constraint violation to zero can be realized at the cost of losing 10.21% optimality. If the decision maker accepts a maximum of 4.53% chance of constraint violation, the budget of uncertainty must be at least 20, i.e., it is sufficient to protect the constraint against only 16% of the uncertain parameters taking all their worst-case values at the same time. It is also interesting to note that even setting the budget of uncertainty at $\Gamma = 20$, i.e., that 20 out of 126 uncertain parameters take their worst-case values all at the same time, results in a significantly low value of violation probability (4.53%), or a high probability of constraint protection against uncertainty (95.47%). In this case, the optimal value is increased by 6.98%, but there is very little effect on the FCV penetration level and the corresponding number of FCVs, since this results in uniform FCV penetration of 2.39%, and an optimal number of FCVs by the end of the planning horizon in all of Ontario of 207,654.

Table 4 presents similar results for the case of considering emission constraints for generation. Observe that setting the budget of uncertainty at Γ=20 results in a reasonable trade-off between optimality and conservatism, since it does not affect significantly the optimal penetration level and the corresponding

Table 3: Sample results of deterministic and robust FCV transition models disregarding emission constraints for generation. (DM: deterministic model; RM: robust model.)

	Γ	Violation probability	Optimal value	Change	Uniform penetration	# of FCVs by 2025
	[-]	[%]	[CAD]	[%]	[%]	
DM	-	-	19,711,182,690	0	2.95	253,799
RM	0	53.55	19,752,896,295	0.21	2.41	207,654
	10	21.13	20,560,656,476	4.31	2.41	207,654
	20	4.53	21,087,436,480	6.98	2.41	207,654
	30	0.49	21,462,267,255	8.88	2.39	205,776
	40	0.03	21,669,378,711	9.93	1.22	104,948
	50	6.3484e-004	21,731,799,724	10.25	1.22	104,948
	60	7.3556e-006	21,753,277,418	10.36	0.76	65,649
	70	3.9479e-008	21,763,392,764	10.41	0.30	25,899
	126	0	21,766,013,701	10.42	0	0

Table 4: Sample results of deterministic and robust FCV transition models including emission constraints for generation.

	Γ	Violation probability	Optimal value	Change	Uniform penetration	# of FCVs by 2025
	[-]	[%]	[CAD]	[%]	[%]	
DM	-	-	19,898,614,370	0	2.95	253,799
RM	0	53.55	19,939,908,389	0.21	2.05	176,795
	10	21.13	20,746,054,029	4.26	2.05	176,795
	20	4.53	21,269,710,333	6.89	2.05	176,795
	30	0.49	21,641,324,147	8.76	1.21	104,155
	40	0.03	21,844,474,815	9.78	0	0
	50	6.3484e-004	21,906,895,830	10.09	0	0
	60	7.3556e-006	21,928,751,579	10.20	0	0
	70	3.9479e-008	21,937,865,105	10.25	0	0
	126	0	21,938,722,324	10.25	0	0

number of FCVs, while the constraint with uncertain parameters is protected with the probability of 95.47% at the cost of losing 6.89% of optimality. In this case, the optimal uniform FCV penetration and the optimal number of FCVs by 2025 in all of Ontario will be equal to 2.05% and 176,795, respectively. It should also be noted that for a very large number of uncertain parameters, the theoretical violation probability for Γ=0 approaches 50%; the slightly higher values in the first rows of Tables 3 and 4 are due to relatively limited number of uncertain parameters.

It should be emphasized that there are several parameters that influence the FCV adoption and transition to a hydrogen economy, such as the costs of FCV and hydrogen production units. These parameters are not considered in the model and the list of uncertain parameters because the proposed optimization model is formulated and solved from the viewpoint of those entities who are involved in policy making for the electricity sector. Thus, this paper suggests a 2.05% electrolytic hydrogen economy penetration in Ontario by 2025 with a "fair" treatment of the involved uncertainties, and based on reasonable values of environmental costs and credits. Although this would be the hydrogen economy that the electricity grid can efficiently support, it is not a penetration level guaranteed to take place, since the costs of FCVs, electrolyzer and hydrogen storage, as well as government support and public acceptance would have a significant impact on the actual penetration levels.

6. Conclusion

The optimal utilization of the electric grid infrastructure during off-peak time periods for the benefit of the transport sector, was studied in this paper. Considering environmental issues, a comprehensive optimization model for the transition to FCVs was developed to determine the optimal electric grid potential to support this type of AFVs in the transport sector for a given planning horizon. The issue of parameter uncertainty was also incorporated into the model. Thus, a methodology based on Monte Carlo simulation was proposed to identify the most influential parameters on the optimal solution. Using these uncertain parameters, a robust optimization approach with the capability of adjusting the level of conservatism/risk was applied to derive robust optimal penetration levels of FCVs into the transport sector. This robust model was finally applied to the real-case example of Ontario, Canada. The results of the robust model demonstrated that with a reasonable trade-off between optimality and conservatism, at least 170,000 FCVs or about 2% of the vehicle fleet can be supported by Ontarios grid by 2025 without any additional grid investments on generation and transmission levels. These results demonstrate the feasibility of developing a hydrogen economy, showing that, with conservative assumptions for technology development, reasonable penetration levels of hydrogen vehicles can be achieved with Ontario's current electric grid configuration and future plans for its enhancement, based on existent hydrogen generation technology.

References

[1] Transport Canada, *Toward Sustainable Transportation*; 2003. URL `http://www.tc.gc.ca/media/documents/policy/discussion.pdf`.
[2] Arico RSM. Measuring the oil vulnerability of canadian cities. Master's thesis; Simon Fraser University; 2007. URL `http://ir.lib.sfu.ca/bitstream/1892/4211/1/etd2765.pdf`.
[3] Turner JA. A realizable renewable energy future. Science 1999;285(5428):687–9.
[4] Ogden J. Hydrogen- The fuel of the future? Physics Today 2002;55(4):69–75.
[5] The Hydrogen Economy: Opportunities, Costs, Barriers, and R&D Needs. Washington, D.C.: The National Academies Press; 2004. URL `http://www.nap.edu`.
[6] McDowall W, Eames M. Towards a sustainable hydrogen economy: A multi-criteria sustainability appraisal of competing hydrogen futures. International Journal of Hydrogen Energy 2007;32(18):4611–26.
[7] Hajimiragha A, Cañizares CA, Fowler MW, Elkamel A. Optimal Transition to Plug-in Hybrid Electric Vehicles in Ontario, Canada Considering the Electricity Grid Limitations. IEEE Trans Ind Electron 2010;57(2):690–701.
[8] Prince-Richard S, Whale M, Djilali N. A techno-economic analysis of decentralized electrolytic hydrogen production for fuel cell vehicles. International Journal of Hydrogen Energy 2005;30(11):1159–79.
[9] Floch P, Gabriel S, Mansilla C, Werkoff F. On the production of hydrogen via alkaline electrolysis during off-peak periods. International Journal of Hydrogen Energy 2007;32(18):4641–7.
[10] Vidueira J, Contreras A, Veziroglu T. PV autonomous installation to produce hydrogen via electrolysis, and its use in FC buses. International Journal of Hydrogen Energy 2003;28(9):927–37.
[11] González A, McKeogh E, Gallachoir B. The role of hydrogen in high wind energy penetration electricity systems: The Irish case. Renewable Energy 2004;29(4):471–89.
[12] Greiner C, Korps M, Holen A. A Norwegian case study on the production of hydrogen from wind power. International Journal of Hydrogen Energy 2007;32(10-11):1500–7.
[13] Martin K, Grasman S. An assessment of wind-hydrogen systems for light duty vehicles. International Journal of Hydrogen Energy 2009;34(16):6581–8.
[14] Ramirez-Salgado J, Estrada-Martinez A. Roadmap towards a sustainable hydrogen economy in Mexico. Journal of Power Sources 2004;129(2):255–63.
[15] Milciuviene S, Milcius D, Praneviciene B. Towards hydrogen economy in Lithuania. International Journal of Hydrogen Energy 2006;31(7):861–6.
[16] Brey J, Brey R, Carazo A, Contreras I, Hernández-Díaz A, Castro A. Planning the transition to a hydrogen economy in Spain. International Journal of Hydrogen Energy 2007;32(10-11):1339–46.
[17] Ball M, Wietschel M, Rentz O. Integration of a hydrogen economy into the German energy system: an optimising modelling approach. International Journal of Hydrogen Energy 2007;32(10-11):1355–68.
[18] Smit R, Weeda M, de Groot A. Hydrogen infrastructure development in The Netherlands. International Journal of Hydrogen Energy 2007;32(10-11):1387–95.
[19] Murray ML, Hugo Seymour E, Pimenta R. Towards a hydrogen economy in Portugal. International Journal of Hydrogen Energy 2007;32(15):3223–9.
[20] Tzimas E, Castello P, Peteves S. The evolution of size and cost of a hydrogen delivery infrastructure in Europe in the medium and long term. International Journal of Hydrogen Energy 2007;32(10-11):1369–80.
[21] Murray ML, Hugo Seymour E, Rogut J, Zechowska SW. Stakeholder perceptions towards the transition to a hydrogen economy in Poland. International Journal of Hydrogen Energy 2008;33(1):20–7.

[22] Contaldi M, Gracceva F, Mattucci A. Hydrogen perspectives in Italy: Analysis of possible deployment scenarios. International Journal of Hydrogen Energy 2008;33(6):1630–42.
[23] Lin Z, Chen CW, Ogden J, Fan Y. The least-cost hydrogen for Southern California. International Journal of Hydrogen Energy 2008;33(12):3009–14.
[24] Ajanovic A. On the economics of hydrogen from renewable energy sources as an alternative fuel in transport sector in Austria. International Journal of Hydrogen Energy 2008;33:4223–34.
[25] Boudries R, Dizene R. Potentialities of hydrogen production in Algeria. International Journal of Hydrogen Energy 2008;33(17):4476–87.
[26] Lee DH, Hsu SS, Tso CT, Su A, Lee DJ. An economy-wide analysis of hydrogen economy in Taiwan. Renewable Energy 2009;34(8):1947–54.
[27] Hajimiragha A, Fowler MW, Cañizares CA. Hydrogen economy transition in Ontario–Canada considering the electricity grid constraints. International Journal of Hydrogen Energy 2009;34(13):5275–93.
[28] Pearce D. The social cost of carbon and its policy implications. Oxford Review of Economic Policy 2003;19(3):1–32.
[29] Yohe GW, Lasco RD, Ahmad QK, Arnell NW, Cohen SJ, Hope C, et al. Perspectives on climate change and sustainability. In: Parry ML, Canziani OF, Palutikof JP, van der Linden PJ, Hanson CE, editors. Climate Change 2007: Impacts, Adaptation and Vulnerability. Contribution of Working Group II to the Fourth Assessment Report of the Intergovernmental Panel on Climate Change. Cambridge, UK: Cambridge University Press; 2007, p. 811–41.
[30] Tol RSJ. The marginal damage costs of carbon dioxide emissions: an assessment of the uncertainties. Energy policy 2005;33(16):2064–74.
[31] Jacobson M. Enhancement of Local Air Pollution by Urban CO_2 Domes. Environmental Science & Technology 2010;44(7):2497–502.
[32] Kantor I, Fowler MW, Hajimiragha A, Elkamel A. Air quality and environmental impacts of alternative vehicle technologies in Ontario, Canada. International Journal of Hyrdogen Energy 2010;35(10):5145–53.
[33] Hajimiragha A. Sustainable convergence of electricity and transport sectors in the context of integrated energy systems. Ph.D. thesis; University of Waterloo; 2010.
[34] Yang C, Ogden J. Determining the lowest-cost hydrogen delivery mode. International Journal of Hydrogen Energy 2007;32(2):268–86.
[35] Gomez-Exposito A, Conejo AJ, Cañizares CA, editors. Electric Energy Systems: Analysis and Operation. CRC Press; 2008.
[36] Motto AL, Galiana FD, Conejo AJ, Arroyo JM. Network-constrained multiperiod auction for a pool-based electricity market. IEEE Trans on Power Systems 2002;17(3):646–53.
[37] Diwekar U. Introduction to Applied Optimization. Norwell, MA: Kluwer; 2003.
[38] Bertsimas D, Sim M. The price of robustness. Operations Research 2004;52(1):35–53.
[39] Bertsimas D, Thiele A. Robust and data-driven optimization: modern decision-making under uncertainty. INFORMS Tutorials in Operations Research: Models, Methods, and Applications for Innovative Decision Making 2006;.
[40] Kall P, Wallace SW. Stochastic Programming. Chichester: John Wiley & Sons; 1994.
[41] Mulvey J, Vanderbei R, Zenios S. Robust optimization of large-scale systems. Operations Research 1995;43(2):264–81.
[42] Kleywegt AJ, Shapiro A. Handbook of Industrial Engineering; chap. 102 Stochastic Optimization. New York: John Wiley and Sons; third ed.; 2001, p. 2625–50.
[43] Sahinidis N. Optimization under uncertainty: state-of-the-art and opportunities. Computers and Chemical Engineering 2004;28(6-7):971–83.
[44] Rubinstein RY, Kroese DP. Simulation and the Monte Carlo Method. New York: Wiley; 2nd ed.; 2007.
[45] Moazeni S. Flexible robustness in linear optimization. Master's thesis; University of Waterloo; 2006.
[46] Sim M. Robust optimization. Ph.D. thesis; Massachusetts Institute of Technology; 2004.
[47] Thiele A. Robust stochastic programming with uncertain probabilities. IMA Journal of Management Mathematics 2008;19(3):289–321.
[48] Beyer H, Sendhoff B. Robust optimization–a comprehensive survey. Computer methods in applied mechanics and engineering 2007;196(33-34):3190–218.
[49] Ben-Tal A, El Ghaoui L, Nemirovski A. Robust Optimization. Princeton, NJ: Princeton University Press; 2009.
[50] El-Ghaoui L, Lebret H. Robust solutions to least-square problems to uncertain data matrices. SIAM J Matrix Anal Appl 1997;18(4):1035–64.
[51] El Ghaoui L, Oustry F, Lebret H. Robust solutions to uncertain semidefinite programs. SIAM journal of optimization 1998;9:33–52.
[52] Ben-Tal A, Nemirovski A. Robust convex optimization. Mathematics of Operations Research 1998;23:769–805.
[53] Ben-Tal A, Nemirovski A. Robust solutions to uncertain programs. Oper Res Lett 1999;25(1–13).
[54] Ben-Tal A, Nemirovski A. Robust solutions of linear programming problems contaminated with uncertain data. Mathematical Programming 2000;88(3):411–24.
[55] Bertsimas D, Sim M. Robust discrete optimization and network flows. Mathematical Programming 2003;98(1):49–71.
[56] Independent Electricity System Operator (IESO), *Ontario Transmission System*; 2009. URL `http://ieso.com/imoweb/pubs/marketReports/OntTxSystem_2009nov.pdf`.
[57] Wendt H, Imarisio G. Nine years of research and development on advanced water electrolysis. A review of the research programme of the Commission of the European Communities. Journal of Applied Electrochemistry 1988;18(1):1–14.
[58] Ouellette N, Rogner HH, Scott DS. Hydrogen from remote excess hydroelectricity. part i: Production plant capacity and production costs. International Journal of Hydrogen Energy 1995;20(11):865–71.
[59] Dutton AG, Dienhart H, Hug W, Ruddell AJ. The economics of autonomous wind-powered hydrogen production systems,.

In: Proc. European wind energy Conference (EWEC'97). Dublin; 1997,.
[60] Amos W. Cost of storing and transporting hydrogen. Tech. Rep. NREL/TP-570-25106; National Renewable Energy Laboratory; Golden, CO; 1998.
[61] Dutton AG, Bleijs JAM, Dienhart H, Falchetta M, Hug W, Prischich D, et al. Experience in the design, sizing, economics, and implementation of autonomous wind-powered hydrogen production systems. International Journal of Hydrogen Energy 2000;25(8):705–22.
[62] Thomas CE, Reardon JP, Lomax FD, Pinyan J, Kuhn IF. Distributed hydrogen fueling systems analysis. In: Proc. of the 2001 DOE hydrogen program review. 2001,.
[63] Simbeck D, Chang E. Hydrogen supply: cost estimate for hydrogen pathways-scoping analysis. Tech. Rep. NREL/SR-540-32525; National Renewable Energy Laboratory; Golden, CO; 2002.
[64] Mignard D, Sahibzada M, Duthie JM, Whittington HW. Methanol synthesis from flue-gas CO_2 and renewable electricity: a feasibility study. International Journal of Hydrogen Energy 2003;28(4):455–64.
[65] Lipman TE, Weinert JX. An assessment of the near-term costs of hydrogen refueling stations and station components. 2006. URL http://repositories.cdlib.org/itsdavis/UCD-ITS-RR-06-03.
[66] Sjardin M, Damen KJ, Faaij APC. Techno-economic prospects of small scale membrane reactors in a future hydrogen fuelled transportation sector. Energy 2006;31(14):2523–55.
[67] Parker N. Optimizing the design of biomass hydrogen supply chains using real-world spatial distributions: A case study using California rice straw. 2007. URL http://repositories.cdlib.org/itsdavis/UCD-ITS-RR-07-13.
[68] Saur G. Wind-to-hydrogen project: electrolyzer capital cost study. Tech. Rep. NREL/TP-550-44103; National Renewable Energy Laboratory; Golden, CO; 2008.
[69] Taljan G, Cañizares CA, Fowler MW, Verbic G. The feasibility of hydrogen storage for mixed wind-nuclear power plants. IEEE Transactions on Power Systems 2008;23(3):1507–18.
[70] Taljan G, Fowler MW, Cañizares CA, Verbič G. Hydrogen storage for mixed wind–nuclear power plants in the context of a hydrogen economy. International Journal of Hydrogen Energy 2008;33(17):4463–75.
[71] Ivy J. Summary of electrolytic hydrogen production, milestone completion report. Tech. Rep.; National Renewable Energy Laboratory; 2004.
[72] Bossel U, Eliasson B, Taylor G. The future of the hydrogen economy: bright or bleak? Cogeneration and Distributed Generation Journal 2003;18(3):29–70. URL http://www.efcf.com/reports/E08.pdf.
[73] Bank B, Guddat J, Klatte D, Kummer B, Tammer K. Non-linear parametric optimization. Birkhäuser Berlin; 1983.
[74] Broadie M. Computing efficient frontiers using estimated parameters. Annals of Operations Research 1993;45(1):21–58.
[75] Moazeni S, Coleman TF, Yuying L. Optimal portfolio execution strategies and sensitivity to price impact parameters. SIAM J Optimization 2010;20(3):1620–54.
[76] Freund RM. Postoptimal analysis of a linear program under simultaneous changes in matrix coefficients. Mathematical Programming Study 1985;24:1–13.
[77] Conejo AJ, Castillo E, Minguez R, Garcia-Bertrand R. Decomposition techniques in Mathematical Programming; chap. 8 Local sensitivity analysis. Springer-Verlag; 2006, p. 304–46.
[78] Fourer R, Gay DM, Kernighan BW. AMPL: A Modeling Language for Mathematical Programming. Pacific Grove, CA: Duxbury Press; 2nd ed.; 2002.
[79] IBM ILOG AMPL version 12.1 User's Guide; June 2009.
[80] MATLAB version 7.9. MathWorks Inc.; 2009. URL http://www.mathworks.com/.